

# DMST Approach for Analysis of 2 and 3 Bladed Type Darrieus Vertical Axis Wind Turbine

Sukanta Roga<sup>1,\*</sup> and Sudhir Kumar Dubey<sup>1</sup>

<sup>1</sup>Department of Mechanical Engineering, Visvesvaraya National Institute of Technology, Nagpur-440010, Maharashtra, India

## Abstract

Wind energy has lately been one of the world's leading outlets of clean energy for producing power in potential environments across the globe. Academics currently undertake numerous analysis practices to improve and refine current wind turbine designs by means of advanced and diverse computational techniques. Various computational tools based on Computational fluid dynamics are available. However, these require a lot of computational time and hardware resources. On the other side, readily accessible basic methods like QBlade are computationally cheap and could be used for efficiency and design analysis of wind turbines on the horizontal and vertical axis. The present study is based on the variable pitch study of vertical axis wind turbine (VAWT) of straight blade NACA0018 airfoil for low speed utilizing QBlade software. The results are validated and compared with the experimental results and it was found to be in good agreement with them for TSR ranging from 1 to 6.

**Keywords:** Green energy, Tip speed ratio, Wind Energy, QBlade

Received on 20 September 2020, accepted on 22 October 2020, published on 27 October 2020

Copyright © 2020 Sukanta Roga et al., licensed to EAI. This is an open access article distributed under the terms of the [Creative Commons Attribution license](#), which permits unlimited use, distribution and reproduction in any medium so long as the original work is properly cited.

Doi: 10.4108/eai.27-10-2020.166771

\*Corresponding author. Email: [rogasukanta@gmail.com](mailto:rogasukanta@gmail.com)

## List of abbreviations

BEM	Blade element momentum
CFD	Computational fluid dynamics
Cd	Coefficient of drag
Cl	Coefficient of lift
Cp	Power coefficient
HAWT	Horizontal axis wind turbine
DMST	Double multiple stream tube
NACA	National advisory committee for aeronautics airfoils
TSR	Tip speed ratio
VAWT	Vertical axis wind turbine

## 1. Introduction

The rapid socio-economic growth and their increasing wages, technology-assisted lifestyles, and better living conditions are the main contributors to the current decades growing cost of energy. Catering for such a strong demand for electricity raises serious problems for the electric power sectors. For long decades non-renewable fuels have become the key sources of electricity generation, but in recent years, being increasingly substituted by renewable energy supplies for eco-friendly development of electricity. There are various alternative sources of renewable energy, e.g., wind energy, biomass energy, solar energy. Solar and wind power are significant forms of green electricity. Ever since the wind has established how to place sails on their vessels and canoes, mankind has used wind strength. Machines propelled by wind have been processing crops and circulating water for quite a while now. This kind of energy has often been readily accessible and not

confined to river banks or fuel sources. With the technological advancements, wind power has seen revitalized applications directly from a locally produced power supply in driving buildings. Wind-driven generators are arriving in huge size ranges this day that can charge batteries or satisfy a vast population's demand for energy. Wind power is a symbol of the transition of the vitality from wind into certain useful forms of vitality with the aid of wind turbines for electrical power production, windmills for mechanical energy, wind siphons for water siphoning exercises/waste, or sails for a ship moving. The energy provided by wind needs modest costs, among many of them [1].

Turbines are mechanically designed to be untouched except under extreme wind conditions but cannot tolerate extreme rotational torques or velocities. Turbines are constructed at cut-out max speed at which the breaks bring the turbine to rest in the absolute lack of which abnormally high aerodynamic torques or rotational speeds result in massive forces on the blades and other sections of the turbine that may destroy the turbine. Different forms of wind turbines can be divided into two categories based on the direction of their axis of rotation; these are horizontal axis wind turbine (HAWT) and vertical axis wind turbine (VAWT). Compared with the lesser-known many other innovations focused on the VAWT, the mainstream mass typically relies primarily on HAWTs. As it is discussed about wider contexts, VAWTs are usually of two forms. VAWT's definition is based on the drag and lift-dependent methodology. In the case of drag-style designs, the drag force is asymmetric in the blade profile and net torque is retained throughout the rotor as the wind flows owing to the force imbalance. The recent information regarding VAWTs, however, has contributed to increased interest in creating a comprehensive analysis between the two [2]. At higher angular velocities of the rotor, the lift-based form has greater efficiency up to the Betz limit, and they come in a variety of shapes and designs. Darrieus rotors generate greater coefficient of strength and are more powerful at higher wind speeds. At lower wind levels they lose the equivalent self-starting capability of a Savonius turbine. Compared with Savonius turbine it is also renowned for producing higher capacity.

Many nations are currently interested in sustainable improvement goals, which require near coordination of 3 dimensions: economic, social, and environmental spheres. In this regard, environmental safety is turning into a top concern. Environmental problems, including international warming, weather change, and air pollutants, negatively affect human beings residing in all nations and territories, especially the poorest and maximum susceptible individuals [3].

The studies' acquired consequences deliver the opportunity to define a brand new technique software of inexperienced power the usage of progressive technologies, sustainable for given power production. For robust operational of PV panels as a part of an available gadget of sustainable street development [4].

High outlet temperature and a large quantity of geothermal fluid extraction should beautify the overall warmth manufacturing. At the same time, low drilling charges are conducive to reducing the geothermal project's payback duration. In this regard, maximum oilfields own terrific capability to generate geothermal energy because they're related to the manufacturing of geothermal fluid from oil reservoirs. Furthermore, deserted oil reservoirs are true capability regions for harvesting and generating geothermal energy, and are maximum favorable due to the fact they're without difficulty retrofitted into geothermal wells [5].

Soaring gas costs and weather extrude are the foremost troubles the arena is facing now. There has long been argued that the industrial gas shares will handiest remain for a few extra time now. Since the human populace relies heavily on the non-renewable assets of power for a lot of its transport, growing options to liquid fuels have emerged as obligatory. Hence, there's international urgency to harness liquid fuels from non-fossil assets [6].

The device's layout and precept, which transforms the kinetic power from stress into electric-powered one, is proposed. The effects of experimental research at the maximum green kind of electric-powered engine's dedication according to the fee of the generated energy output are presented. The processing of empirical studies has performed essential mathematical physics strategies, particularly the trapezoid method [7].

## 2. Literature review

Diverse scientists have used different computational methods to examine VAWT's outputs. Several scientific experiments and statistical work have been performed to deduce the aerodynamics viability of VAWTs. The Momentum process, including stream tube models, tends to be a simple yet powerful tool for maximizing research performance. Previous analyzes are compatible with experimental findings on the implementation of these structures. The DMST models have the benefit of prompt prognosis coupled with strong success in the study of VAWTs. This model is widely used by academics in the performance review of VAWTs. It is also accurate for the estimation of VAWT behaviors [8].

In the literature survey, the BEM model is being used in research projects for the examination of Darrieus-type VAWT output and other parameters with straight blade configuration. In addition to this, for aerodynamic efficiency, a thorough evaluation of the effects of spatial and functional parameters was also worked out. The effects of various parameters are often analyzed including blade airfoil shape, number of blades, chord duration, and free wind speed. The findings of this study allowed VAWT designers to use a realistic, cost-effective, and time-efficient method to offer interpretation of their output. The study gives the implication of this methodology for the current investigation. One more such research involves the BEM method which is as stated before a numerical computations

methodology in performing pitch control analysis over a HAWT with a blade radius of 37m and power capacity of 2.1MW. The effects of tower effect were studied regarding the decrement of relative velocity by 3%. The end results of the analysis gave good accord close to the outboard region of the blade compared to the inboard zone for greater than rated wind velocity. Data analysis was carried out for different speeds in active pitch monitoring for 2.1MW wind turbines with a rotor diameter of 95m and a hub height of 80m with on-site location within India [9]. In a separate analysis, two reference points in the upper part of the turbine cycle are established for a quick and precise estimation which continuously alters AOA in two reference points upstream of the turbine blades based on the velocity flux results. The detailed analysis and simultaneous comparison of the functioning of the performance VAWT turbine based on a fixed pitch and the sinusoidal variable pitch was carried out. The conclusion of the analysis was the enhancement of the complete performance of the VAWT when variable pitch was used. It gave vitals for the usage of variable pitch in VAWT [10]. The researcher depends on the BEM hypothesis for the HAWT configuration, considering the impact of the wake on the rotor plane in the general structure. This impact is assumed to be smaller, in order to support the upgrade of information predicting the consequences of the wake on the rotor plane. The proposed numerical model in this work is an expansion of the BEM strategy, utilizing the Glauert's model adjusted for the breeze turbine structure. The numerical model introduced in this paper presents an elective device for the breeze turbine structure, exceptionally for moderate rotors, when it is anticipated in its principle structure the most broad condition that relates the enlistment factors in the rotor plane and the wake, in view of the Glauert's hypothesis and BEM model, that was altered here to foresee the conditions set by equations [11].

Specific researchers now have investigated the fluctuating pitch techniques for growing the power coefficient of the straight-bladed VAWT as a method to boost turbine efficiency. Instead of increasing the largest torque, the azimuthal angle band of the blade was extended with the maximum aerodynamic torque. The approach utilized gives a contour of pitch angle constructed for the blade functioning at the graded tip speed ratio (TSR) analogous to the peak power coefficient of the Fixed pitch (FP)-VAWT. The proposal utilizes the DMST model and Prandtl's loss factor for estimation of losses incurred in the blade tip. The research covered various aspects such as drag, lift, angle of attack, torque, power output, etc. And their computations were done for different TSR's: 4, 4.5, 5, and 5.5 both for fixed and variable pitch type turbine. The approach followed by the paper gives an improvement of 18.9% in the peak power coefficient of VAWT. The improved results are due to the widened zone of work. Apart from this enhancement, it is observed that the new pitching method improves the performance at TSRs which are larger than the given optimal values, and improvement of torque generation is also observed [12].

An empirical analysis of the impact of the preset angle on the output of a VAWT was performed in the different research. The test carried out featured a three-bladed H-Darrieus VAWT. The flow solutions were overcome by means of a commercial software tool ANSYS CFX 13 CFD file. The Turbine with NACA0015 airfoil profile is used in the model case for comparison and zero pitch angles were utilized for analytical comparison. The analysis was evaluated at three-pitch angles with TSR ranging from 1 to 2.2. The maximum value of both speed ratios and wind speeds is found for the pitch angle rated at -6°. In order to know the influence of pitch the pressure coefficient variations throughout the upwind blade and streamlines at various azimuthal angles were also evaluated. Based on the above study, the present work is focused on the analysis of two-bladed Darrieus VAWT for the variable pitch model with the help of QBlade software. Its work is focused on the effects of the flow near the edge of the turbine blade and its contribution to the lift phenomena of the turbine rotor. The analysis of straight-bladed turbines is carried out based on BEM methodology using QBlade open source software and the effect of variable pitch on power and thrust parameter of VAWT is examined [13].

An analytical solution of aerodynamic unsteady and steady flow over the airfoil of the 2-D VAWT model was carried out. A model design and working conditions of the paper were taken through the literature surveys of the Darrieus-type wind turbine. The research majorly focuses on the analysis of steady and unsteady lift and drag coefficients over the airfoil blade. On comparing the outcome of the lift force coefficient attained amidst, two separate modeling gives indicative variance in the static stall regions [14].

The numerical analysis has been extensively used for the analytical examination as seen through literature surveys. In a study of two-bladed Darrieus VAWT at a regulated TSR of 5.0, the aerodynamic loading over the blade as compared to derived results. As a result of this paper gave instantaneous wake profile generated at the back of the rotor and instantaneous forces over the blade surfaces. Aerodynamic wake generated at the rear section of the rotor is visualized through the use of streak lines [15]. A comprehensive scrutiny of past and current research of the H-Darrieus VAWT turbine against the prospect of design specification which includes turbine solidity, blade profile, pitch angle, etc. was performed. With precise focus kept over the critical difficulties faced while designing a turbine with self-starting capabilities. The variety of major research field approaches used for examining the turbine was covered in it [16].

### 3. Methodology

Academics are gradually utilizing CFD tools such as ANSYS Fluent and Open-FOAM for the efficiency and interface review of VAWTs. This has already been stated, nevertheless, that CFD approaches require considerable hardware infrastructure and time-consuming resources. The BEM-based numerical

models are good replacements to the CFD methodologies. Furthermore, a publicly accessible programming device with a user-friendly interface is desired, which can effectively integrate diversified airfoils. QBlade is among such free software and was also selected for the current research project [17].

Several academics have subsequently used different numerical methods to forecast the wind turbine output for its own advantages and disadvantages. For a small-scale VAWT, extensive details on both of these statistical approaches may be retrieved from Methods centered on momentum such as the Single Stream Tube Model, the Double Stream Tube Model, and the Double Stream Tube Model was the easiest and fastest amongst the others. The current research is performed using the QBlade software which utilizes the DMST approach for the analytical purpose for VAWT. The appropriate airfoil was selected based on the literature review. The below steps were followed using QBlade to reach the results.

### 3.1. Theoretical formulation

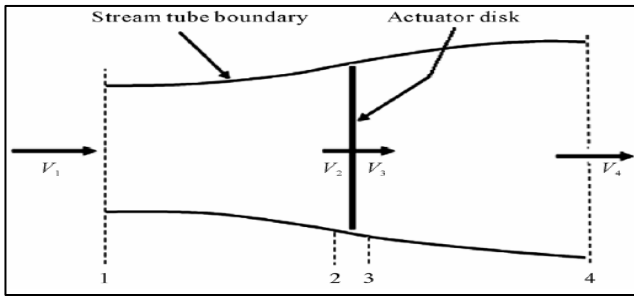


Figure 1. Actuator disk model [16]

Based on the literature survey following numerical results are based upon [18]. The power is the same and the reverse of the torque,  $T$ , which would be the wind energy on the wind turbine. Through the protection of linear momentum with a one-dimensional, incompressible, time-invariant wave, the thrust is equivalent to, and opposed to, the increase in air stream momentum:

$$T = V_1(\rho AV)_1 - V_4(\rho AV)_4 \quad (1)$$

Where,  $\rho$  is the air density,  $A$  is the cross-sectional area,  $V$  is the air velocity and the subscripts indicate values at numbered cross-sections as indicated in figure 1.

For steady-state flow,

$$(\rho AV)_1 = (\rho AV)_4 = \dot{m} \quad (2)$$

where,  $\dot{m}$  is mass flow rate;

Therefore,

$$T = \dot{m}(V_1 - V_4) \quad (3)$$

The torque is favorable and the velocity underneath the rotor,  $V_4$ , is smaller than the velocity of the open stream,  $V_1$ . There is no job at either part of the turbine rotor.

$$V_2 = \frac{V_1 + V_4}{2} \quad (4)$$

The axial induction factor is known as ‘a’ as the marginal decline in wind speed between the free stream and the rotor plane.

$$a = \frac{V_1 - V_2}{V_1} \quad (5)$$

$$V_2 = V_1(1 - a) \quad (6)$$

$$V_4 = V_1(1 - 2a) \quad (7)$$

The axial thrust on the disk is

$$T = \frac{1}{2} \rho AV_1^2 [4a(1 - a)] \quad (8)$$

Non-dimensional thrust coefficient is given as following

$$C_T = \frac{T}{\frac{1}{2} \rho AV^2} \quad (9)$$

### 3.2. Study of straight bladed Darrieus VAWT

General Mathematical Expressions for Aerodynamics [16]

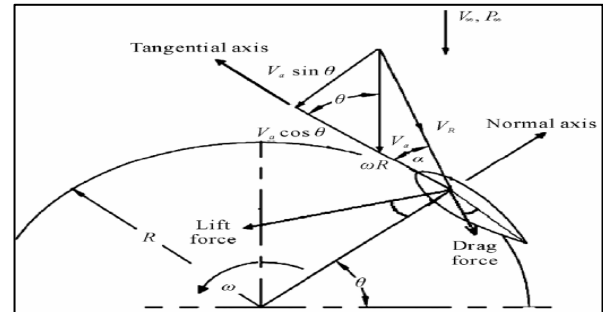


Figure 2. Airfoil velocity and force diagram [16]

Straight bladed Darrieus type VAWT is the simplest type of wind turbine which is utilized for analytical purposes. The aerodynamic research over these turbines is still very complex. There are variations in velocities of the flows in the upstream and downstream sections of the Darrieus-type VAWTs.

The basic mathematical formulas at a given position of the blade are listed below with reference to figure 2. Where ‘a’ is the induction factor and ‘ $\lambda$ ’ is the tip speed ratio of the turbine.

From the figure 2, the angle of attack is expressed as:

$$\tan \alpha = \frac{V_a \sin \theta}{V_a \cos \theta + \omega R} \quad (10)$$

Non-dimensionalizing the equation 17 by dividing numerator by  $V_\infty$

$$\alpha = \tan^{-1} \left( \frac{(1-a) \sin \theta}{(1-a) \cos \theta + \lambda} \right) \quad (11)$$

The normal and tangential coefficients is given as

$$C_n = C_L \cos \alpha + C_D \sin \alpha \quad (12)$$

$$C_t = C_L \sin \alpha - C_D \cos \alpha \quad (13)$$

where,  $C_L$  lift coefficient and  $C_D$  drag coefficient for an angle of attack  $\alpha$ . The instantaneous thrust force  $T_i$  on one single airfoil for any  $\theta$  is

$$T_i = \frac{1}{2} \rho V_R^2 (hc) (C_t \sin \theta - C_n \cos \theta) \quad (14)$$

where,  $h$  is blade height and  $c$  is blade chord length. The instantaneous torque  $Q_i$  on one single airfoil at certain  $\theta$  is

$$Q_i = \frac{1}{2} \rho V_R^2 (hc) C_t R \quad (15)$$

### 3.3. Simulation setup

A simulation was performed utilizing QBlade tools [22] to measure the performance of the airfoil. The airfoils have a four-digit sequence of the Regional Airfoils Consultative Committee, NACA0018. The symmetrical airfoil is chosen because it has a low starting torque. QBlade program was included in this research article to perform the conceptual study of wind turbine blades. The research analysis should concentrate on the wind turbine with a vertical axis. A description of wind turbine vertical axis (VAWT) study using QBlade tools into three groups are;

- Designing the blades of the wind turbine.
- The designing and simulating the rotor of the designed wind turbine.
- The simulation of the complete wind turbine.

### 3.4. Airfoil selection

The airfoil chosen for the current analysis as well for validation is NACA0018. The selection of airfoils in QBlade is quite easy. The NACAXXXX airfoils can readily be generated inside QBlade. The selection is based on an extensive literature survey.

### 3.5. XFOIL direct analysis

To perform VAWT efficiency analyzes in QBlade, XFOIL is primarily used to produce aerodynamic coefficients before deployment. XFOIL direct analysis was conducted for the current analysis to produce aerodynamic coefficients for  $-10^\circ$  indicating  $+10^\circ$ . The transformations of the boundary layer were regulated by the Ncrit value in XFOIL that is a feature of the turbulence intensity levels.

### 3.6. 360° polar extrapolation

The lift and drag coefficients were required for the conduction of the performance analysis of a VAWT. To do that first, the lifting and drag coefficients derived from XFOIL could be modeled for  $\alpha$  lying between  $0^\circ$  and  $360^\circ$  utilizing the correct model. QBlade currently has two post-install versions that are:

- Extrapolation to Montgomery
- Viterna-Corrigan Post-Stall Model

As per the QBlade Guidelines, First is necessary to use the subtle Montgomery extrapolation. Additionally, the post-stall model Viterna- Corrigan, which is preferred in automotive applications, is also available. The Montgomery extrapolation has been used for the existing analysis.

### 3.7. Rotor design and Simulation

Selection of the revisions to the DMS algorithm and the parameters of the simulation are carried out when describing a rotor simulation. The collection of a set of TSR (tip speed ratios) and the phase for simulation is performed after a description of the simulation. A simulation of the rotor is still dimensional. This is presumed that the free stream speed is unitary and that the rotor size and height for calculation are normalized. To progress a simulation of a wind turbine, a rotor blade must be defined and the file should be present during the runtime. The file should be there in the database of the QBlade. The parameters should be pre-defined which are correlated to the wind rotor. The parameters that define a turbine are rotor blade cut-in and cut-out wind speeds, turbine offset, fixed and variable losses related to the flow.

The cut-in and cut-out wind speed determines the turbine's spectrum of operating wind speeds. The turbine offset enables a rotor to be positioned at varying heights in which the inflow speeds differ because of the wind profile induced by friction. Set and dynamic damages are liable for the failure of gear and generators. The rotor configuration is shown in table 1 and illustrated in figure 3 and figure 4.

Table 1. Rotor specification

Airfoil	NACA0018
Number of blades	2 and 3
Blade height	1 m
Rotor radius	1 m
Chord	0.2 m
Density of air	1.225 kg/m <sup>3</sup>
Viscosity of air	0.000016547 kg/(m-s)
Epsilon	0.001
Relaxation factor	0.3
Reynolds number	50000

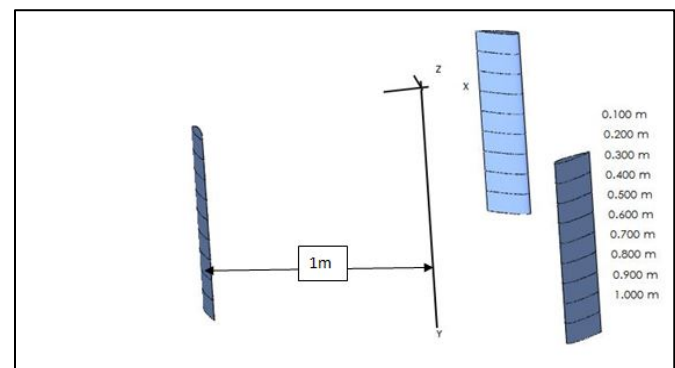


Figure 3. Two-bladed turbine model

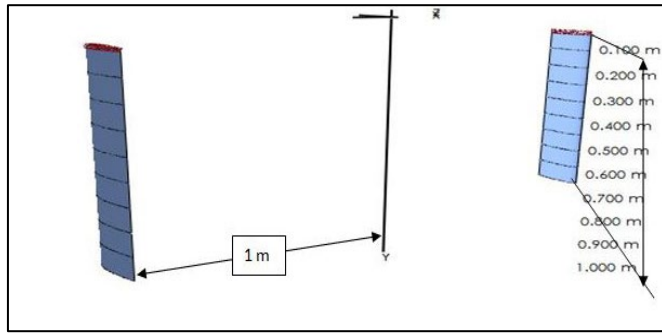


Figure 4. Three-bladed turbine model

## 4. Results and discussion

### 4.1. validation

Airfoils utilized in the wind turbine for low speed should have a high lift coefficient and comparatively low drag coefficient. The QBlade open source software is used in the analysis of the project. The validation is carried out by comparing the lift and drag coefficient of results obtained by earlier CFD runs to that of the current work in QBlade to validate the following work in the used software. The initial study was carried out in ANSYS CFD tool for the comparison of the result of  $C_l$  and  $C_d$  values. The results gave good agreement with the current study. Even comparative analysis with the previous CFD papers the results have good accord. The lift on an airfoil is primarily the result of its angle of attack and shape. The literature referred for validation contrasts findings for aerodynamic loads and wake profiles produced by implementing models of turbulence such as: the normal  $k-\epsilon$ ; the RNG  $k-\epsilon$ ; the Realizable  $k-\epsilon$ ; and the SST  $k-\omega$ . These all simulations are contemporary models and can be observed in many other CFD Simulation protocols as mentioned e.g. in the ANSYS Fluent documentation theory guide (ANSYS, version: 16.0).

Figure 5 to 7 shows the computational domain, meshing of the domain and meshing near the blade respectively. In figure 3 is the computational domain setup for the validation of QBlade with the CFD model and existing paper in the CFD domain, here  $d_i$  ( $20c$ ) and  $d_o$  ( $40c$ ) are the upstream and downstream distance of the domain,  $W$  ( $40c$ ) is the width of the domain, with free stream velocity of 7 m/s. Some of the essential factors of the mesh influencing the analytical methods are: the size of the square region, the edge size of the profiles, the number of layers of structured mesh, the pattern of increase of structured mesh, the pattern of increase of unstructured mesh and the density of the very first surface in a direction perpendicular to the wall (wall  $y+$ ). The authors CFD tests are tested for four models of turbulence: the SST  $k-\omega$ , the  $k-\epsilon$ , the RNG  $k-\epsilon$ , and the Realizable  $k-\epsilon$ . However, for the purpose of the validation result of only one model that is the Realizable  $k-\epsilon$  is taken and the results are extrapolated from the paper for values shown in the table.

Table 2 and 3 gives the  $C_l$  and  $C_d$  values, it shows the close resemblance of QBlade results with CFD results and referred paper [20] results. When oriented at a suitable angle, the airfoil deflects the oncoming air, resulting in a force on the airfoil in the direction opposite to the deflection. This force is known as aerodynamic force and can be resolved into two components: lift and drag. Numerical calculations for wind turbine aerodynamic in preliminary analysis were performed utilizing ANSYS-Fluent, which is a commercial CFD analytics program focused on the finite volume process.

In CFD analysis, Reynolds-average Navier-Stokes (RANS) equations have used the Realizable  $k-\epsilon$  turbulence interface with contour rectification. Second-order upwind discretization was also used in space. The rotor radius is taken as 1m and chord length as 0.2 m. Since the current study is for the slow speed wind turbine with variable pitch analysis in the range of -10 degree to 10 degree. The validation is carried out for angle of attack ranging from 0 degree to 5 degrees only for Reynolds number 40,000. QBlade being gives faster results hence the further work was carried out in this system itself whose models for two-blades and three-blades have been kept in the later part of this discussion for different parameters.

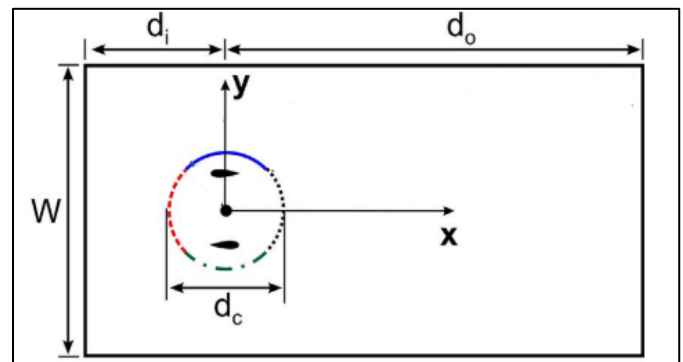


Figure 5. CFD domain

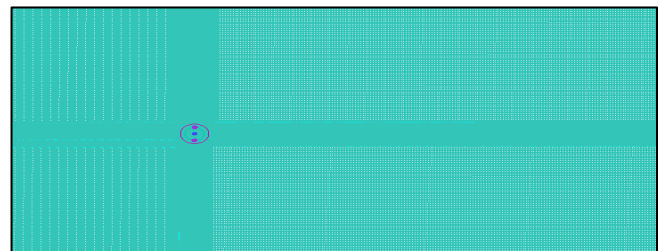


Figure 6. CFD domain in ANSYS Fluent

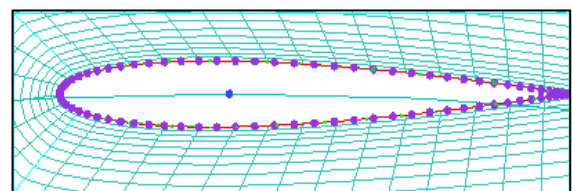


Figure 7. Close view of the domain

The values deviate due to the usage of different airfoil in the methodology of paper and that with this current study. However close resemblance is observed in terms of value obtained from QBlade evaluation and referred paper for Cd and Cl values for the chosen airfoil NACA0018. The current paper is based on NACA0018 airfoil since its vast application in wind turbine sector and its symmetrical profile make it easy to compute. The result gave good agreement with the results from the referred paper of Rogowaski. Thus it can be concluded that the model developed shows close tally with the previous results for Cl vs alpha plot and Cd vs alpha plot. Hence further results can be deduced as a model gives accurate results

Table 2. Validation results for Cl

Angle of attack (degrees)	Result referred paper [15]		Result from paper [19]	CFD results	QBlade results
	Realizable k- $\epsilon$ results	Experimental results			
1	0.10	0.10	0.10	0.12	0.15
5	0.54	0.58	0.64	0.66	0.78

Table 3. Validation results for Cd

Angle of attack (degrees)	Result referred Paper [15]		CFD results	QBlade results
	Realizable k- $\epsilon$ results	Experimental results		
1	0.025	0.019	0.029	0.021
5	0.030	0.022	0.038	0.023

Hence, in the further work to evaluate the performance of distinct small VAWT models for equivalent swept area and rotor solidity, an aerodynamic analysis will be made available. The DMST model built using QBlade resulted in a satisfactory outcome as it contributed to efficiency changes by using a variable pitch approach. In the following section, numerical and simulation result has been discussed of variable pitch of NACA0018 airfoil section of Darrieus type VAWT for two-bladed and three-bladed models. An aerodynamic study will be developed in order to analyze the performance of two and three-blade model of small VAWT models for the identical swept region and rotor solidity. In the model rotor diameter, chord length, rotor height is kept constant. Furthermore, the measurements suggested using the NACA0018 airfoil indicate increased rotor performance when beginning TSRs (at low rotor rates, reducing VAWT start-up problems), but more pronounced restriction in the usage of wind energy at low to moderate wind speeds, typical of the urban community. The distinction was also rendered with respect to weights, adjusting several of the rotor characteristics such as blade number (2 and 3), TSR (using symmetric blade NACA0018), and wind speed.

The latest analogy was rendered on aerodynamic rotors loads, which often offer rise to concerns of both rotor efficiency and key structural specifications. No torque losses from the support (struts) system and therefore no thrust working on the shaft was put into account to concentrate only on the impact in design at the blade. Further analysis was carried utilizing the QBlade, the 3D model of the rotor was rendered in it, and all the analysis was carried in the same both for the two-blade and three-blades turbine models

## 4.2. Results

### 4.2.1. Analysis of two-bladed model

Figure 10 is the two models used for the analysis. DMST model developed using QBlade gave the result that comes out to be satisfactory as it led to improvement of performance when a variable pitch approach was employed. In the model rotor diameter, chord length, rotor height is kept constant.

#### 4.2.1.1. Cl/Cd vs Azimuthal angle

The analysis was carried for five different TSR namely 3, 3.5, 4, 4.5, 5, and wind speed of 4m/s. The plots were obtained for Cl/Cd vs Azimuthal angle. Figure 8 to figure 17 illustrates the shows the variation of the lift and drag ratio over the length of the turbine. In this figure 8, figure 10, figure 12, figure 14, figure 16 shows the trend near the edges and it is observed that the contribution to lift is very less from the top and bottom edges of the turbine and they contribute to large losses. Improvement in the design mostly the better twist angle and changing the blade angle near the edges can help in improving the lift near the edges. The TSR 3.5 gives the improved power output. Figure 8, figure 11, figure 13, figure 15 and figure 17, gives the mid-portion contribution of turbine rotor to the lift. The maximum contribution to power generation is from the midsection of the turbine. The curve is observed to be trapezoidal in both the upwind and downwind section of the rotor. The lift drag ratio contribution is Maximum from this portion of the rotor. The best result gets for TSR 4.0. For above this tip speed ratio, a slack is noted in the downwind part and for below tip speed ratio, the slack is observed in the upwind direction. The variable pitch gives the trapezoidal curve and it is aimed but has the curve similar to it, as it improves the power contribution of the turbine as a whole.

The DMST evaluation gives quick and precise results of the analysis carried for the two-blade model. The study led to emphasis more on the further need for investigation required for the study of different approaches needed to develop the shape of the blade near the top and bottom section of the blade, to reduce the overall losses incurred by the turbine. Approaches such as the blade twisting, thickness variation will lead to variation in the performance of the turbine model. An in-depth analysis is still needed to be carried out to ascertain the impact of these factors over the efficiency of the turbine power

generation which is beyond the scope of this research. The current result limits the findings to how the top and bottom sections contribute to the power domain of the turbine, and suggesting methods to improve the same. As given below figure

signifies and as mentioned above the share distribution as majorly contributed by the middle portion of the turbine blade and major loss contribution by the top and lower section of the turbine.

#### 4.2.1.1.1. TSR 3

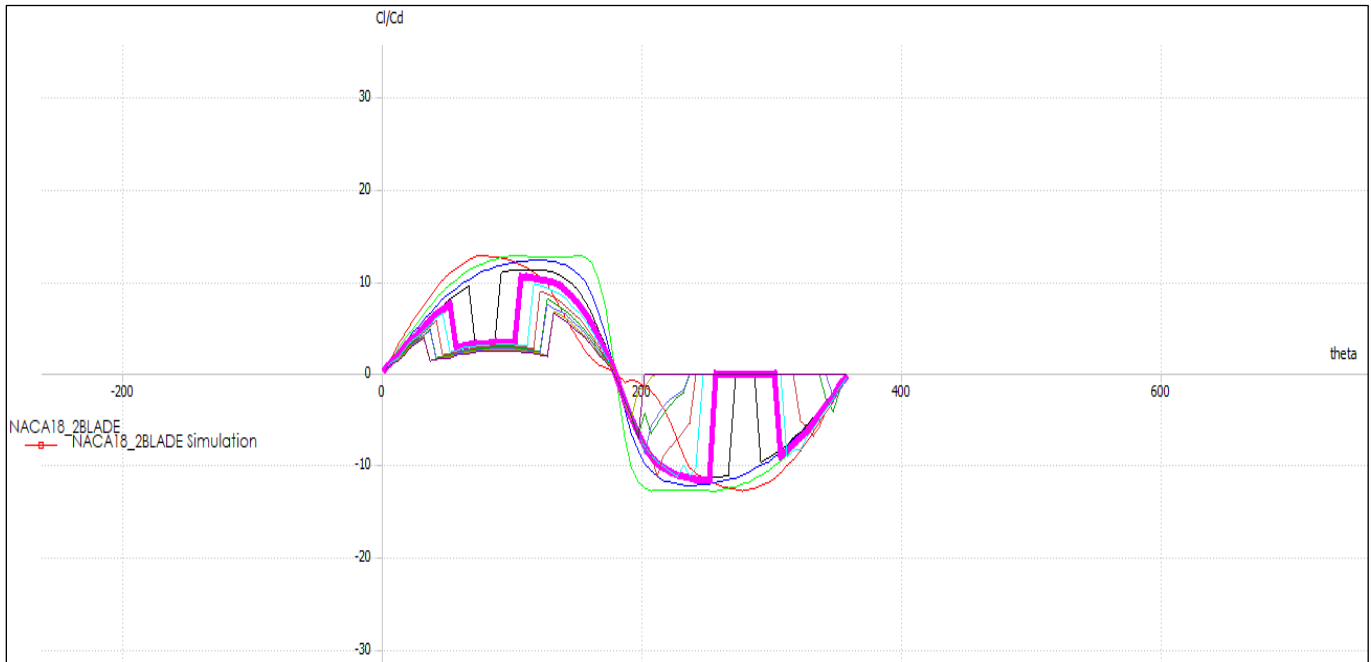


**Figure 8.** Cl/Cd vs theta plot of top-section for TSR 3

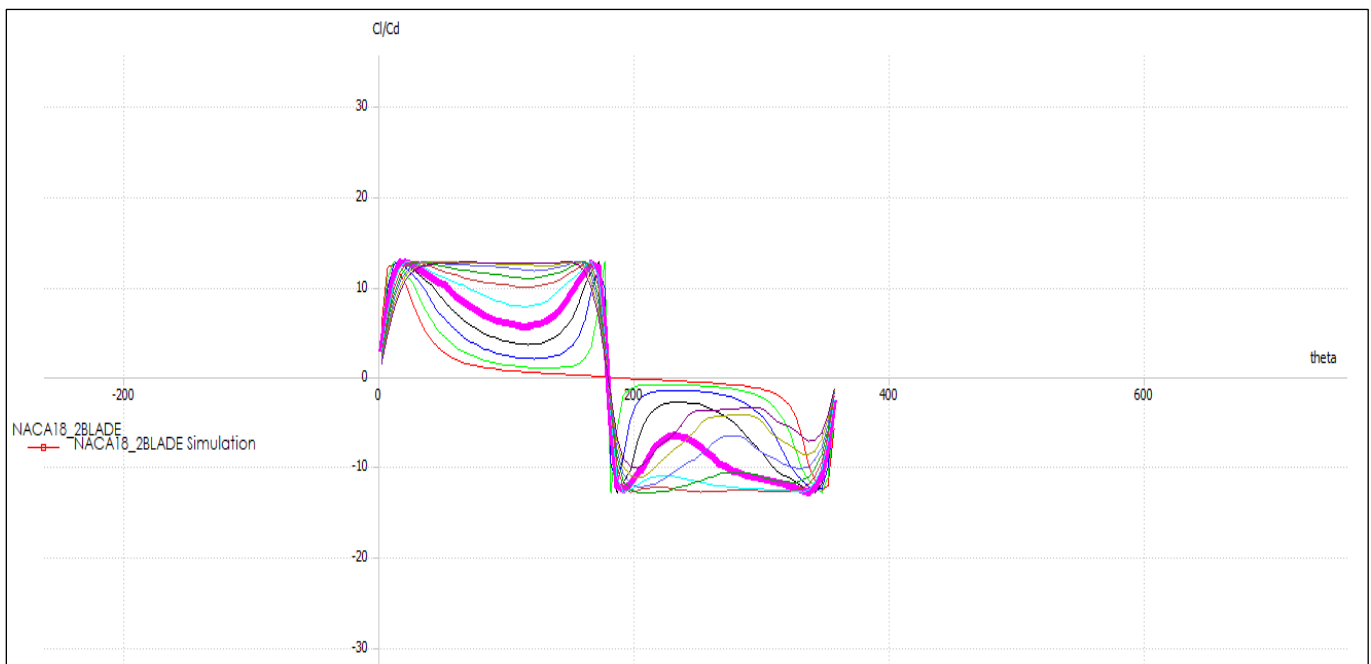


**Figure 9.** Cl/Cd vs theta plot of mid-section for TSR 3



#### 4.2.1.1.2. TSR 3.5

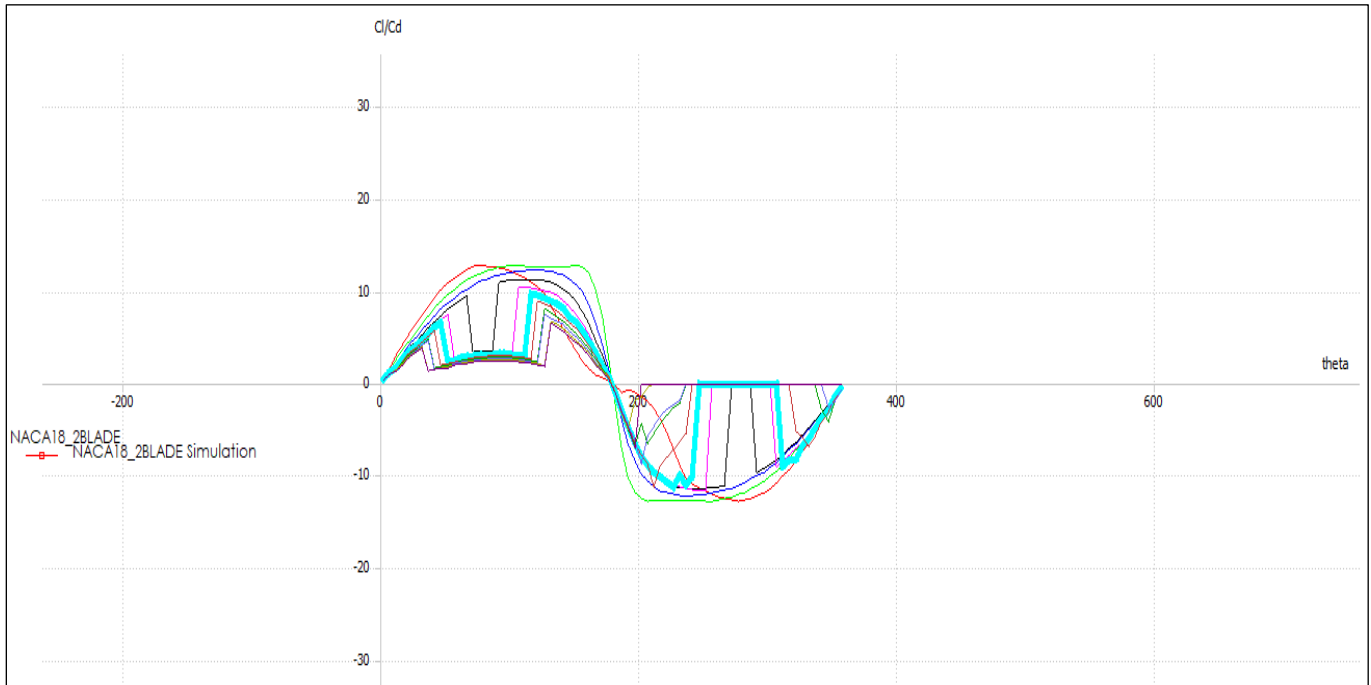


Figure 10. CI/Cd vs theta plot of top-section for TSR 3.5

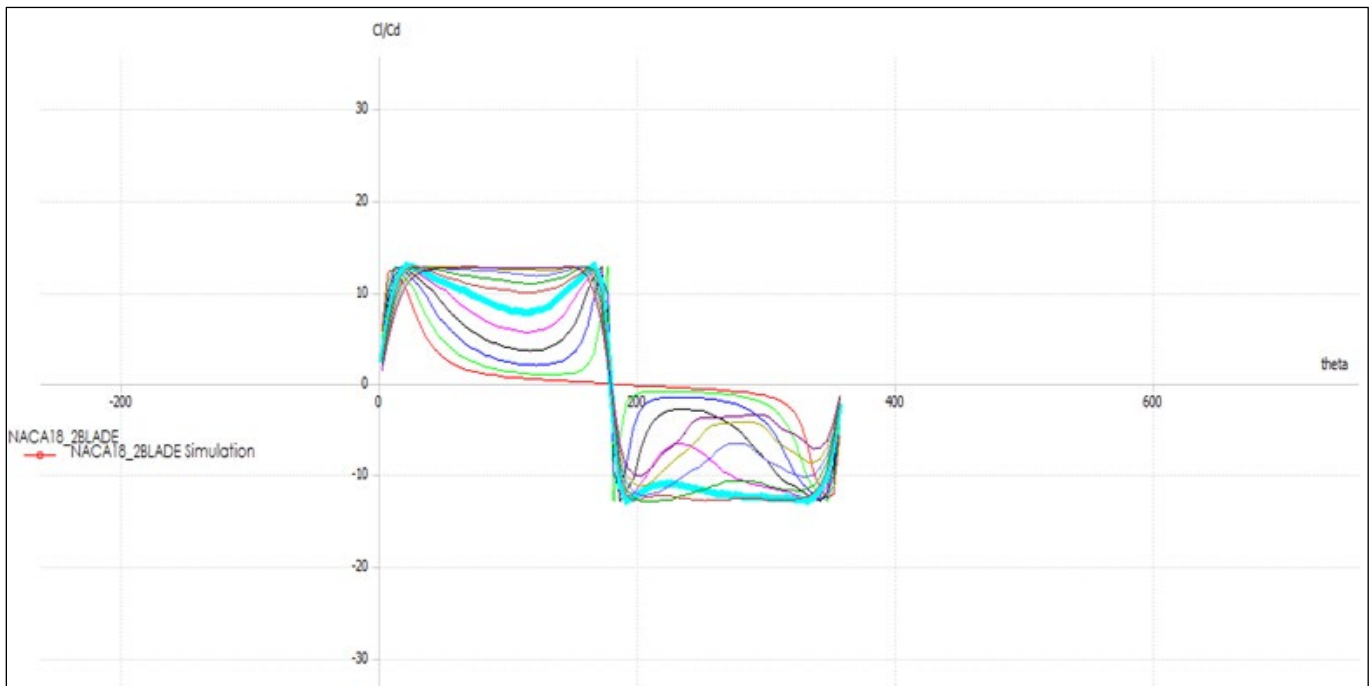


Figure 11. CI/Cd vs theta plot of mid-section for TSR 3.5

### 4.2.1.1.3. TSR 4

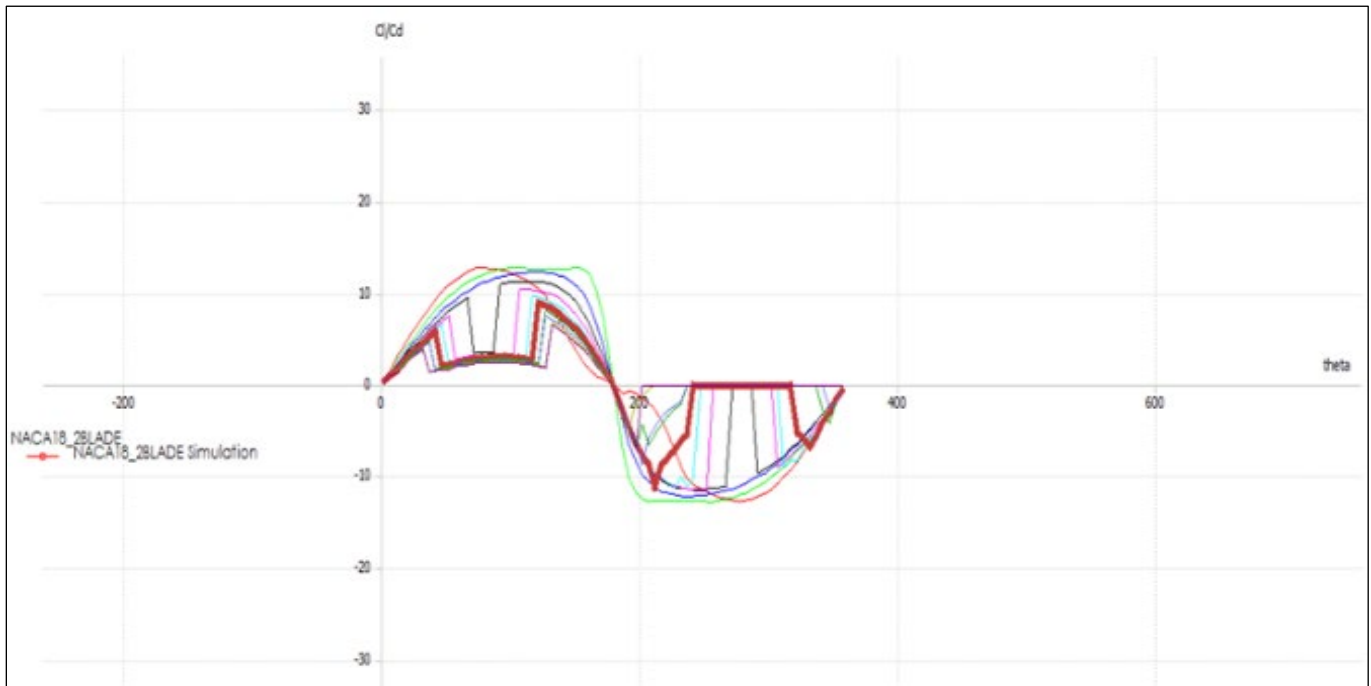


Figure 12. Cl/Cd vs theta plot of top-section for TSR 4

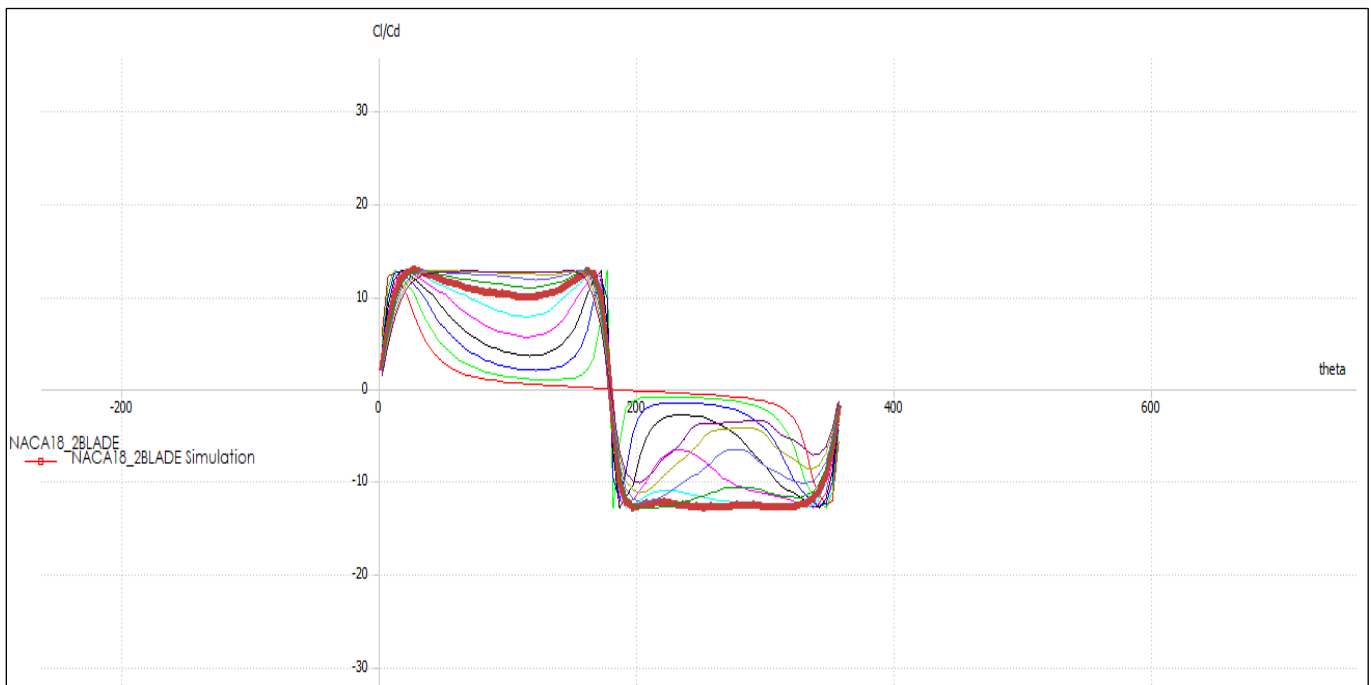


Figure 13. Cl/Cd vs theta plot of mid-section for TSR 4

#### 4.2.1.1.4. TSR 4.5

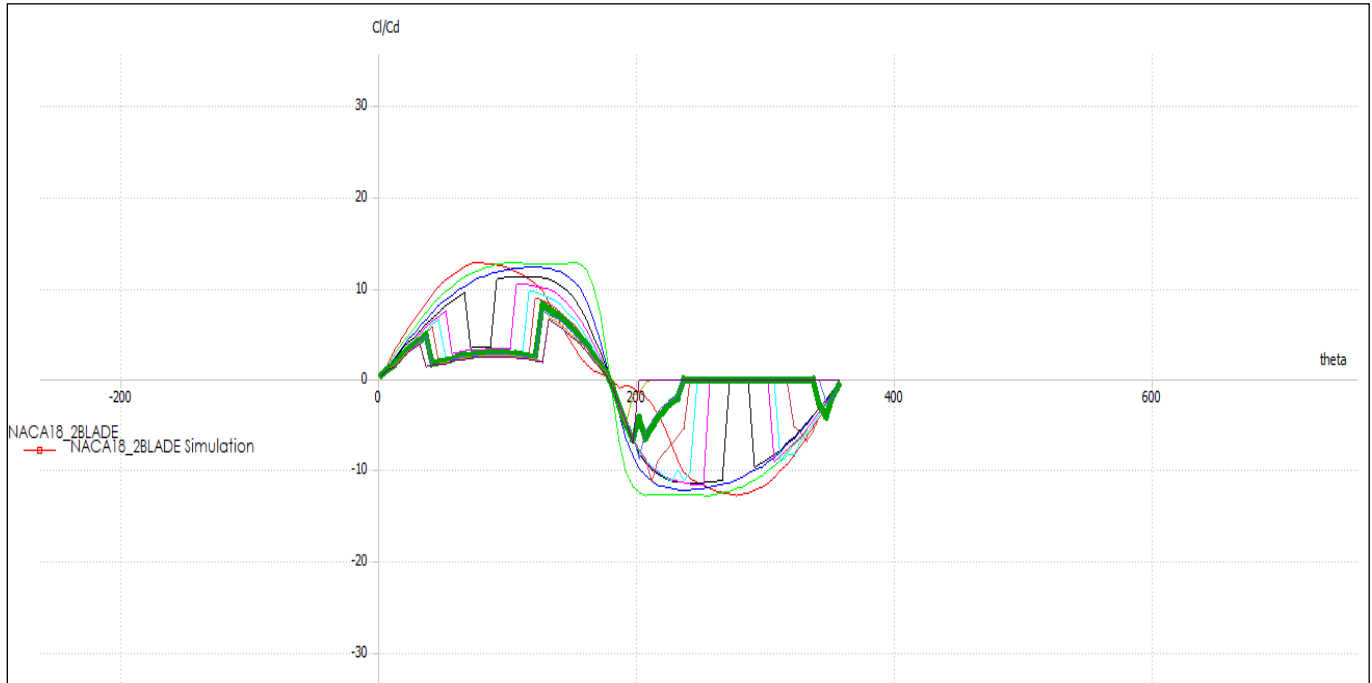


Figure 14. Cl/Cd vs theta plot of top-section for TSR 4.5

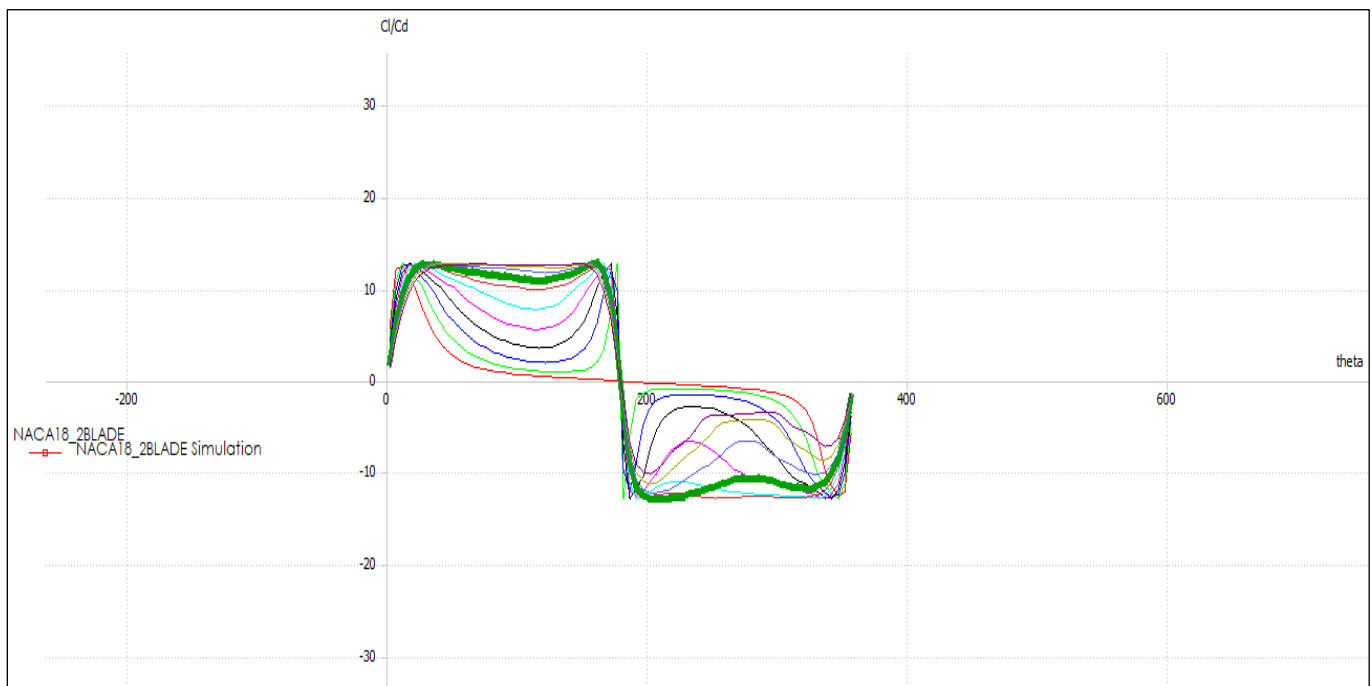
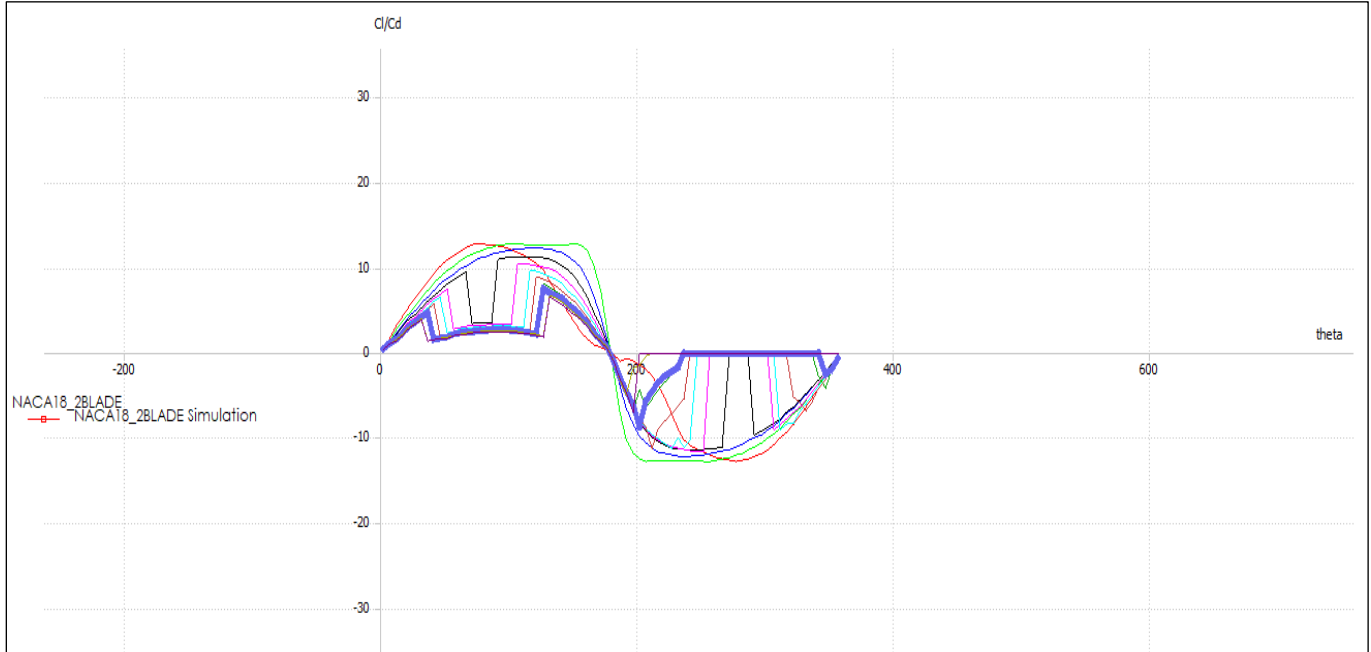
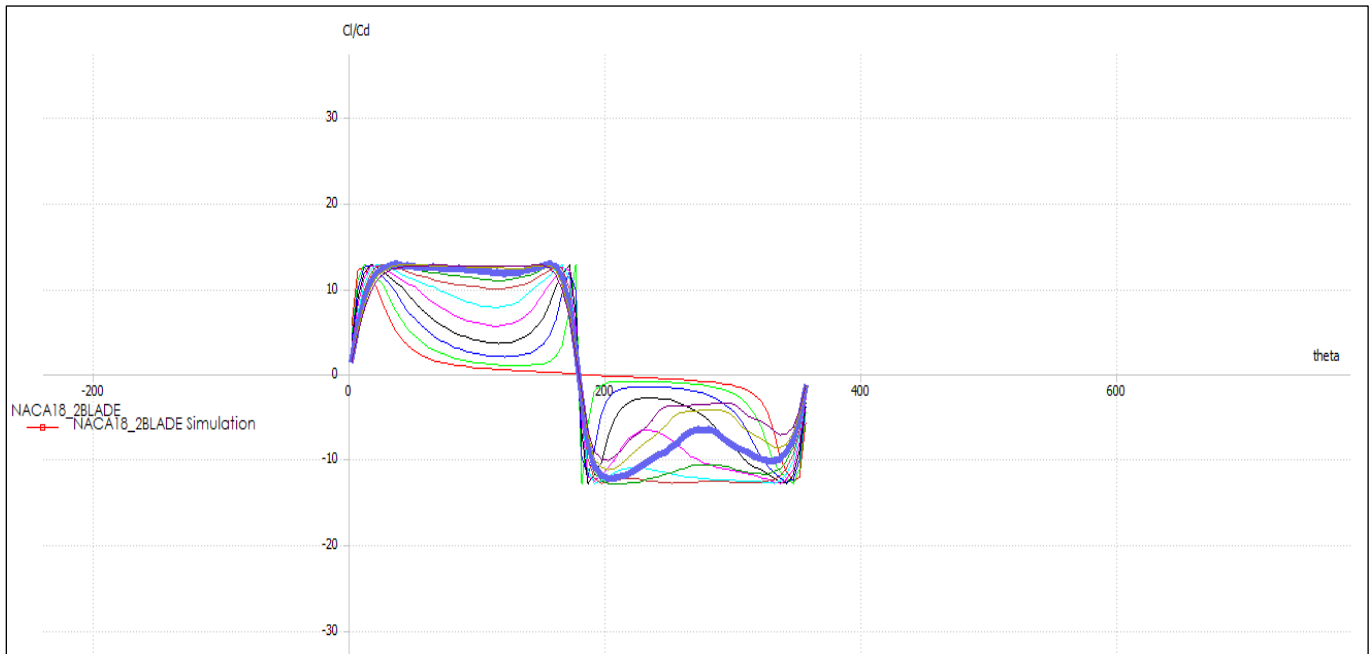


Figure 15. Cl/Cd vs theta plot of mid-section for TSR 4.5

#### 4.2.1.1.5. TSR 5



**Figure 16.** CI/Cd vs theta plot of top-section for TSR 5



**Figure 17.** CI/Cd vs theta plot of mid-section for TSR 5

#### 4.2.1.2. Cm vs alpha

Figure 18 gives the illustration of the coefficient of moment,  $C_m$  versus angle of attack,  $\alpha$ . The  $C_m$  values increase for zero degree to five degrees for both positive and negative angle of pitching and on further increasing the pitching value there is

a decrement in the moment value. It can be deduced that the output is better for a variable pitch value for angle between negative five degrees to positive five degrees and the turbine as an optimum operation in this range of pitch.

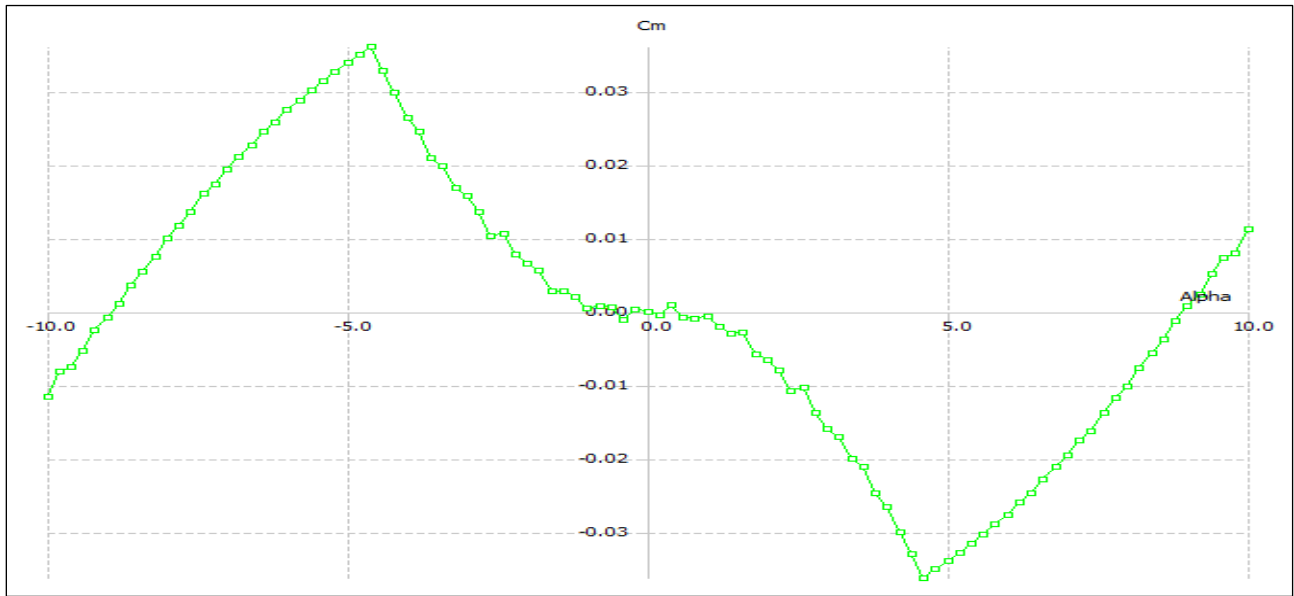


Figure 18. Cm vs Alpha for 2 Bladed VAWT

#### 4.2.1.3. Cp vs TSR

Figure 19 illustrates the graph between the coefficient of power and tip speed ratio from TSR 1 to TSR 6. There is an increase in the Cp value from TSR one to TSR 3.5 and declination in Cp is observed beyond the 3.5 TSR. This curtails the working

TSR should be between 3 TSR to 3.5 TSR for the optimum results from the turbine. The results showed improved performance compared to the experimental results of the paper referred [21].

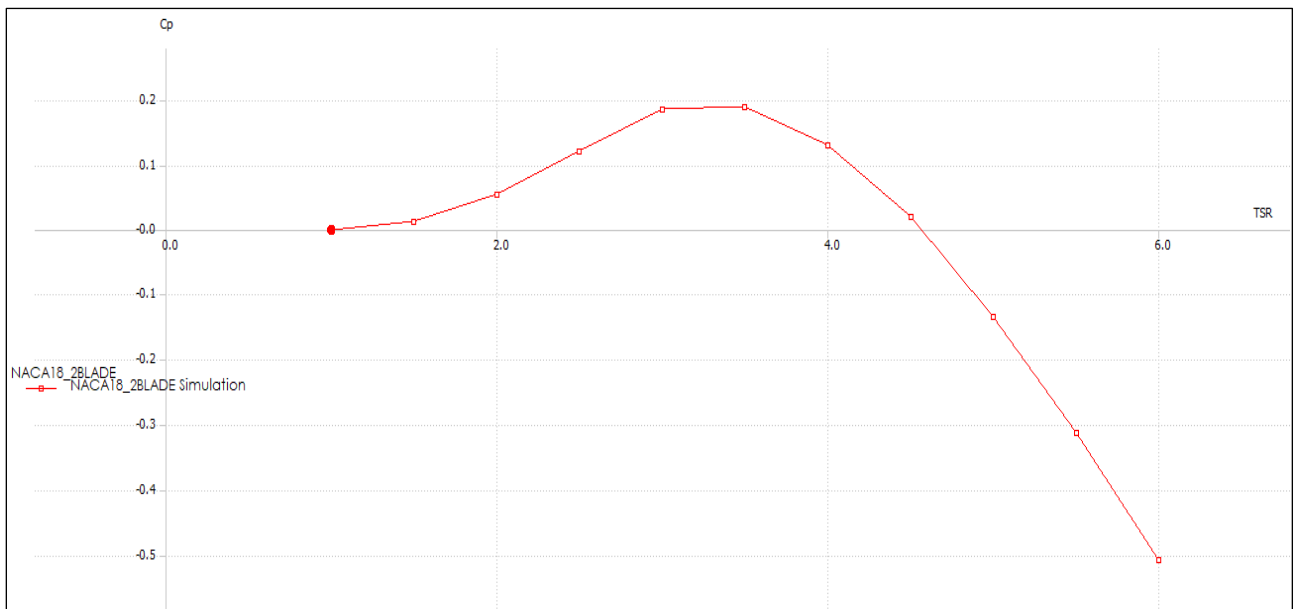


Figure 19. Cp vs TSR for 2 Bladed VAWT

#### 4.2.1.4. Power vs wind speed

Figure 20 illustrates the curve between powers developed by the turbine to wind speeds. The turbine runs for low wind speed. The speed is incremented from 3 m/s to 8 m/s. It can be noted

that there is an increase in power output with an increase in wind speed for the variable pitch model.

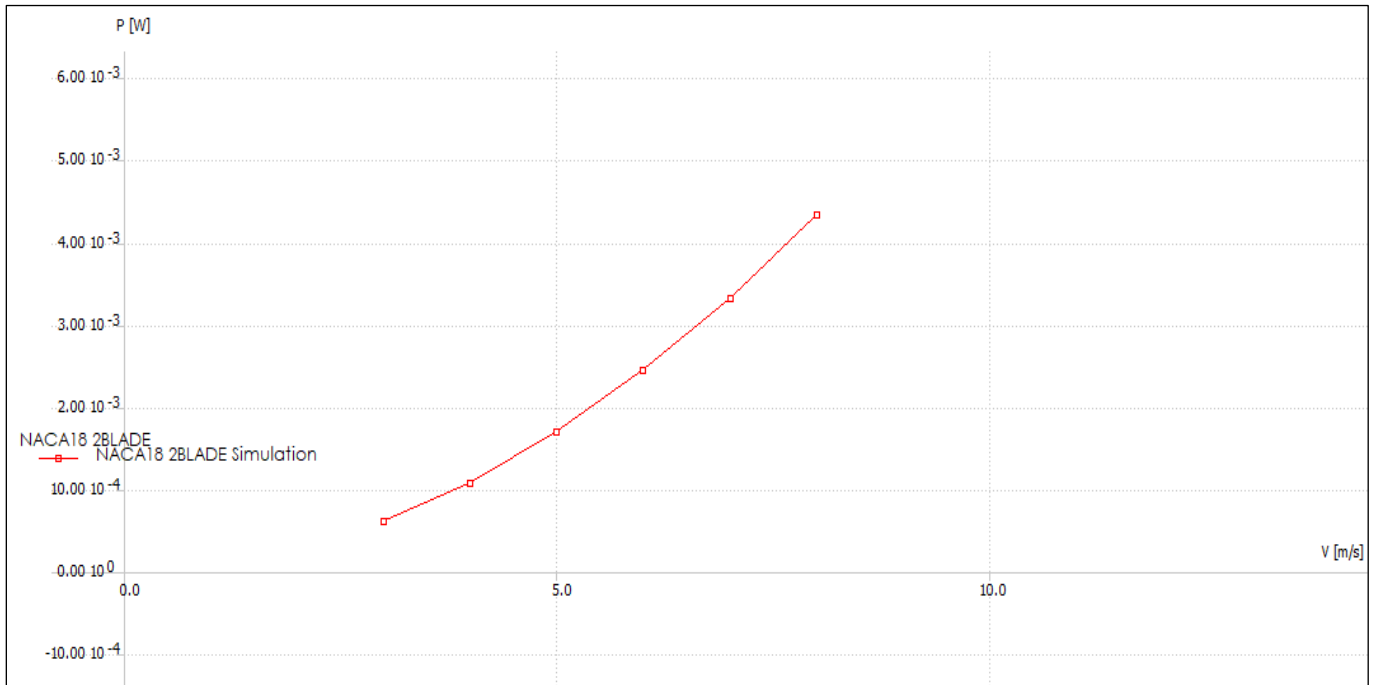


Figure 20. Power vs wind speed for 2 Bladed VAWT

#### 4.2.1.5. Torque vs wind speed

Figure 21 depicts the plot between torques and wind speed. The plot gives an increasing trend of the torque with an increase in wind speed. At a speed of 3 m/s, the torque produced is 0.06

Nm and increases to the value of 0.42 Nm at a wind speed of 8 m/s.

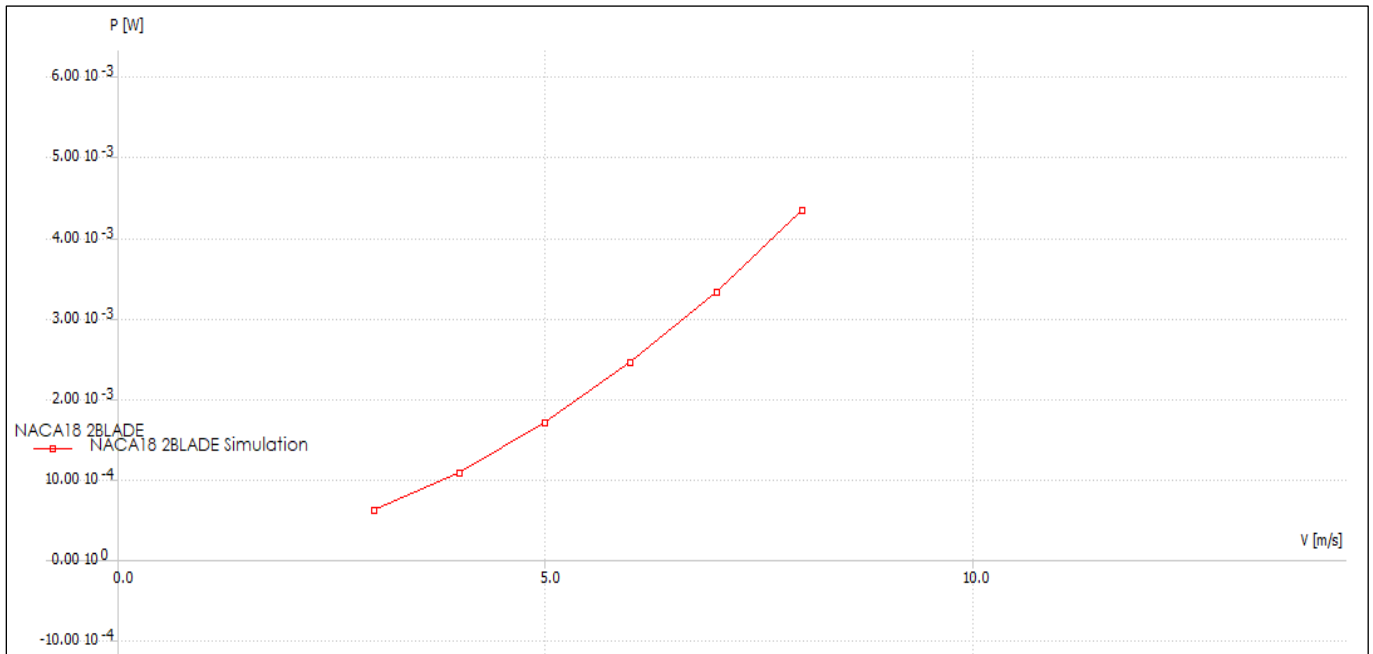
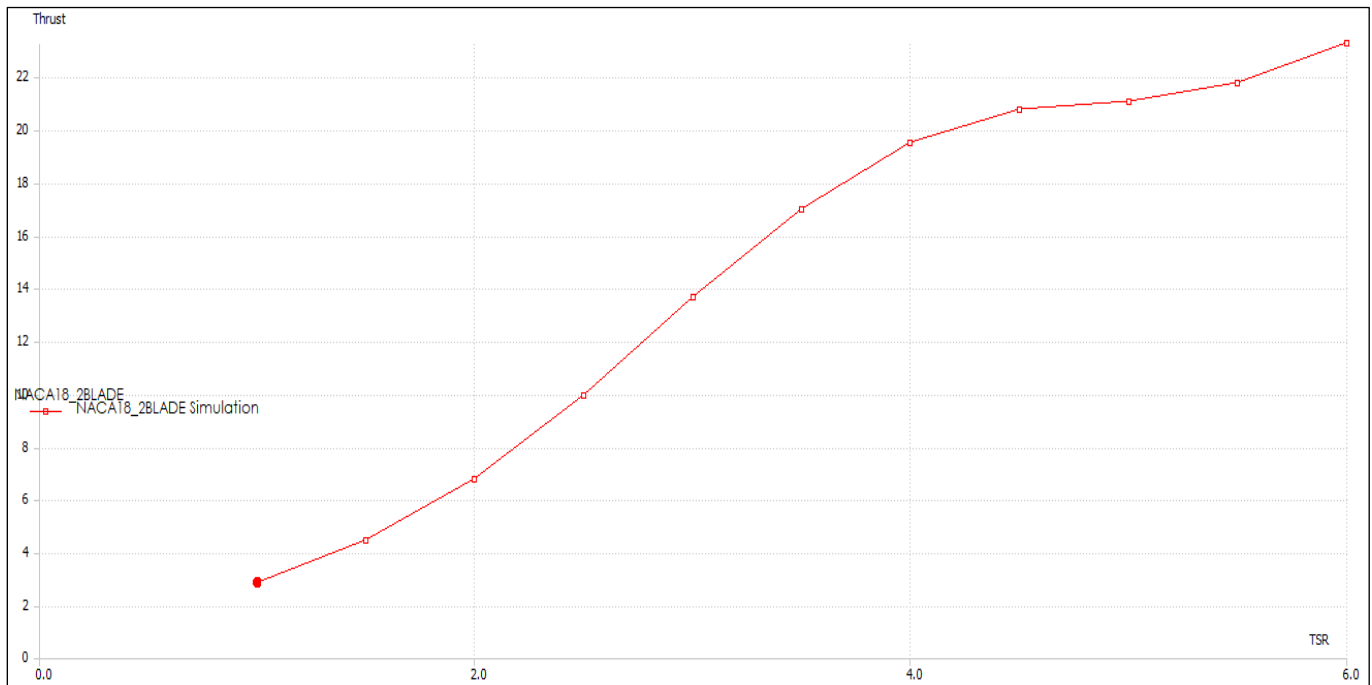


Figure 21. Torque vs wind speed for 2 Bladed VAWT



**Figure 22.** Thrust vs TSR for 2 Bladed VAWT

#### 4.2.2. Analysis of Three-bladed model

Figure 4 is the three-blade model used for the analysis. The DMST model built using QBlade resulted in a satisfactory outcome as it contributed to efficiency changes by utilizing a variable pitch method. The rotor height is held fixed in the diameter of the layout rotor, the chord frequency. 1.2.1  $Cl/Cd$  vs Azimuthal angle.

The analysis was carried for five different TSR namely 1, 2, 3, 4 and 5 wind speeds of 4m/s. The plots were obtained for  $Cl/Cd$  vs Azimuthal angle. Figure 23 to figure 40 illustrates the shows the variation of the lift and drag ratio over the length of the turbine. For different TSR, each top-section, middle-section, and bottom-section contribution to lift has been given

in graphical form respectively. On analysis of graphs, it can be inferred a similar trend as that of a two-bladed turbine that is from the area near the edges of the top and bottom of the turbine section the contribution to lift is very less to power generation as lower lift is generated in this section also they contribute of large losses as seen in two-blade turbine section as well. Improvement in the design mostly the better twist angle and changing the blade angle near the edges can help in improving the lift near the edges. During working under the operating range of TSR 3 and TSR 4, the turbines give a better optimum contribution to lift which implies better power output and better functioning of the turbine in this range of TSRs.

### 4.2.2.1. TSR 1

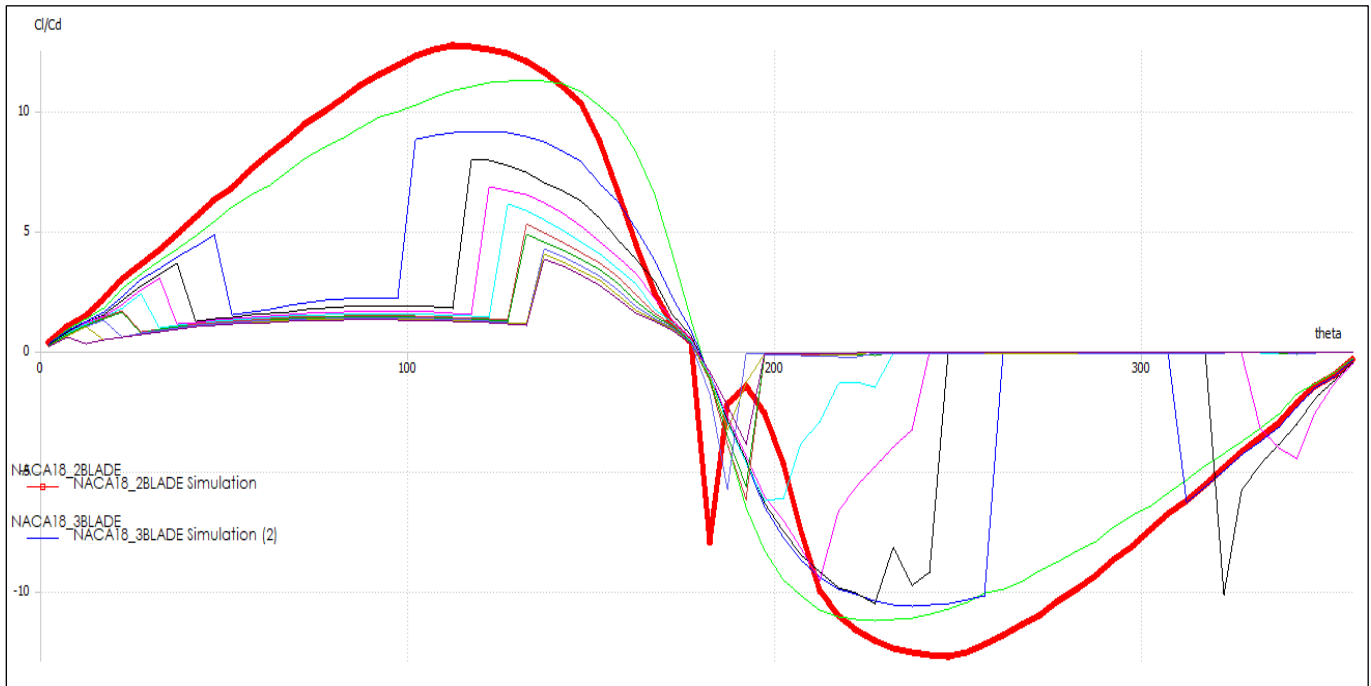


Figure 23. Cl/Cd vs theta plot of top-section for TSR 1

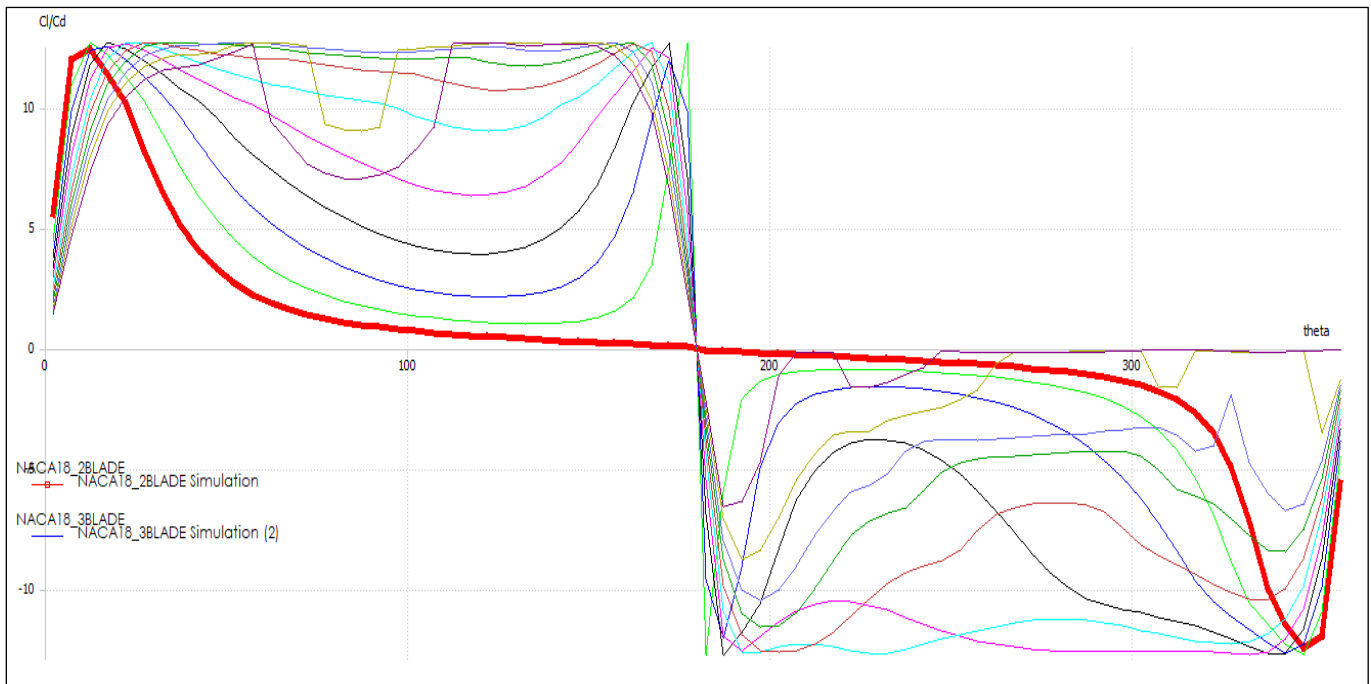


Figure 24. Cl/Cd vs theta plot of mid-section for TSR 1



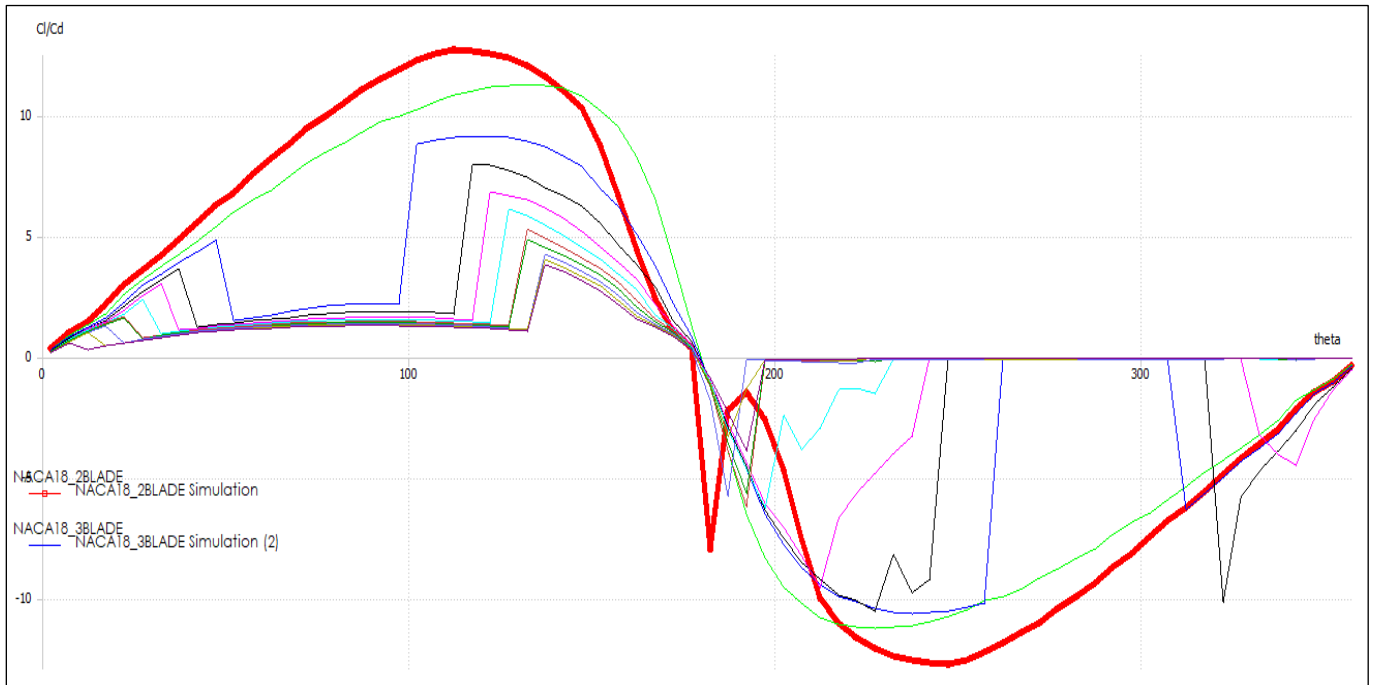


Figure 25. CI/Cd vs theta plot of bottom-section for TSR 1

#### 4.2.2.2. TSR 2

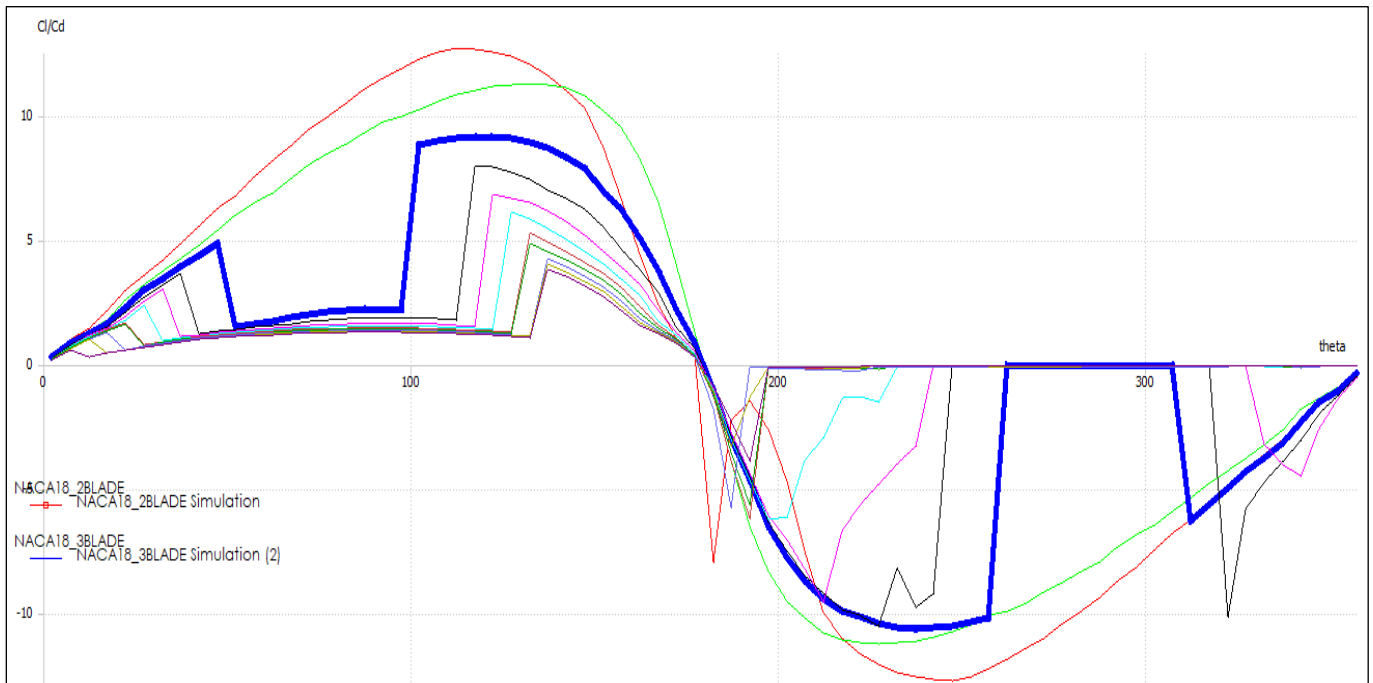


Figure 26. CI/Cd vs theta plot of top-section for TSR 2

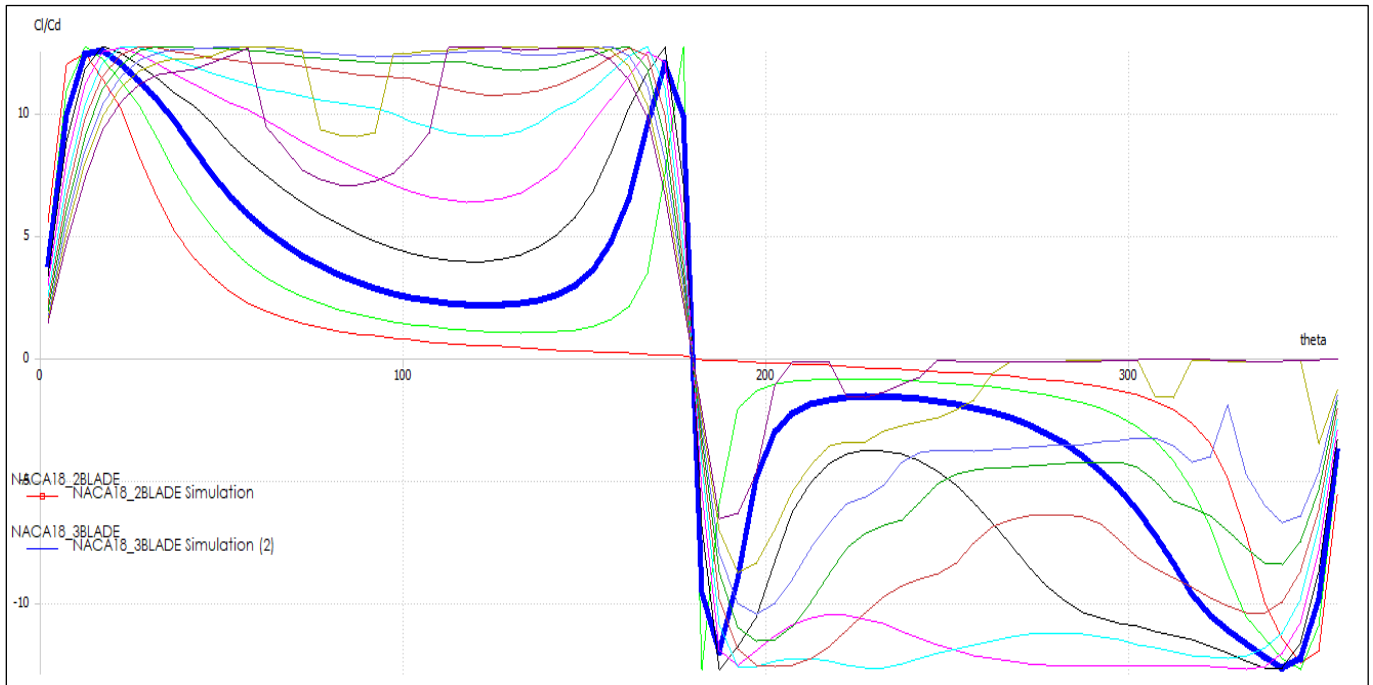


Figure 27. Cl/Cd vs theta plot of mid-section for TSR 2

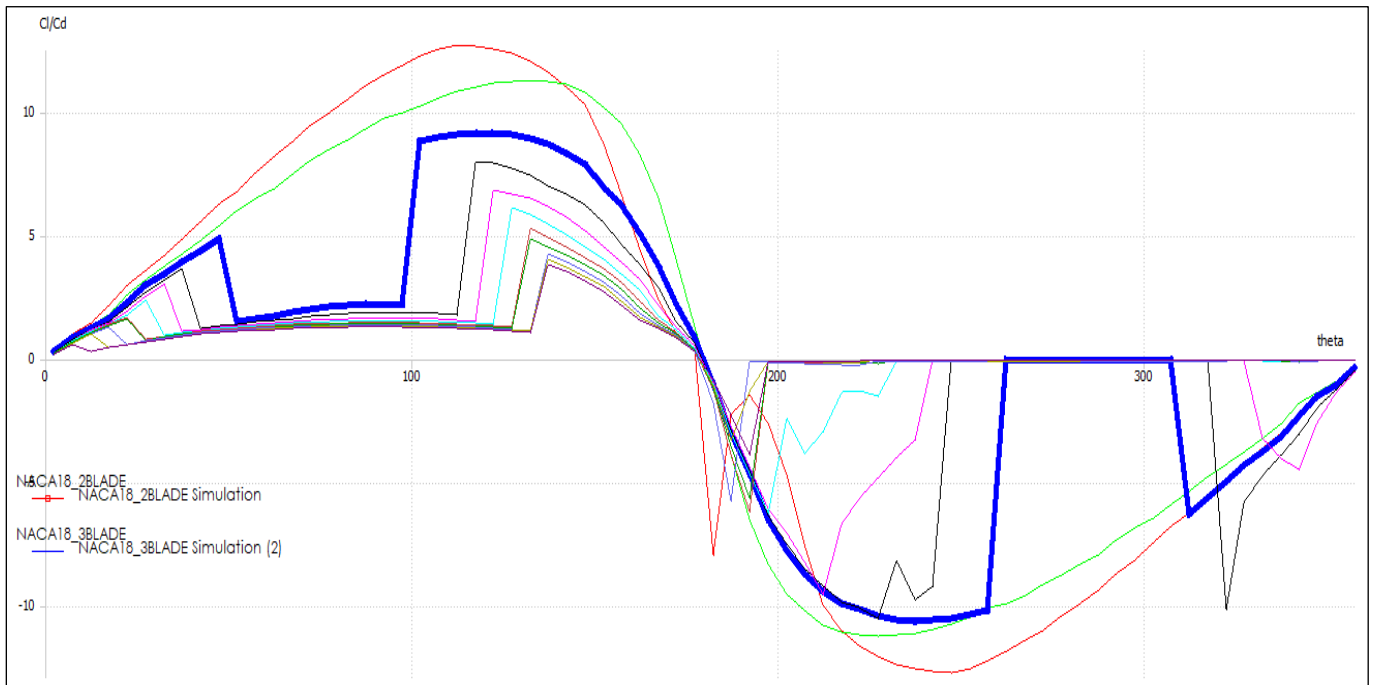
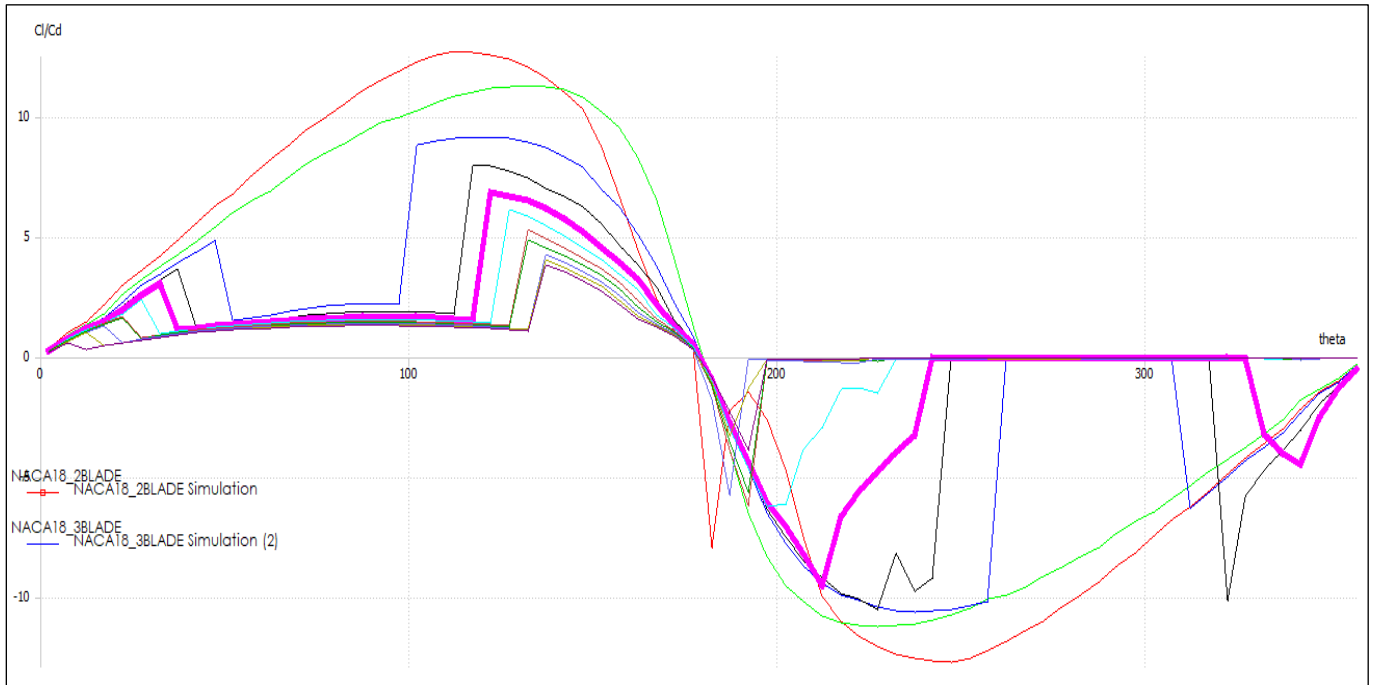
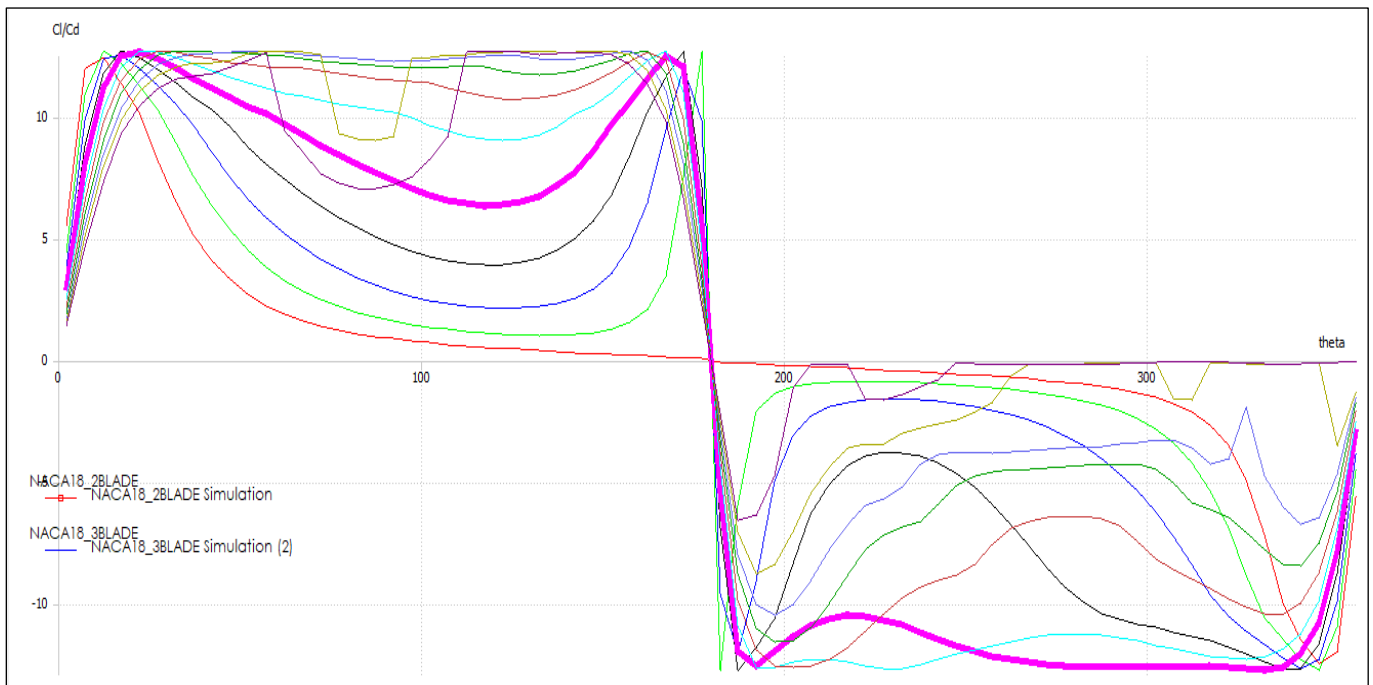


Figure 28. Cl/Cd vs theta plot of bottom-section for TSR 2

### 4.2.2.3. TSR 3



**Figure 29.** Cl/Cd vs theta plot of top-section for TSR 3



**Figure 30.** Cl/Cd vs theta plot of mid-section for TSR 3

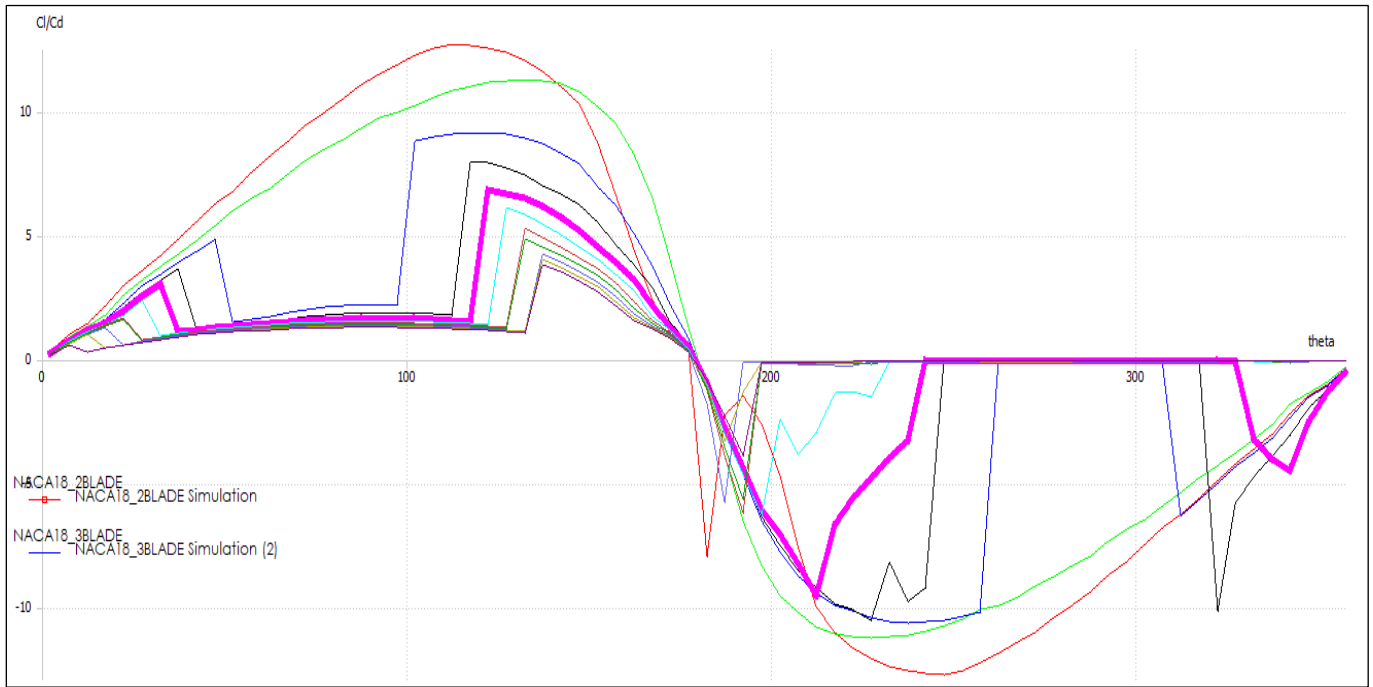


Figure 31. Cl/Cd vs theta plot of bottom-section for TSR 3

#### 4.2.2.4. TSR 4

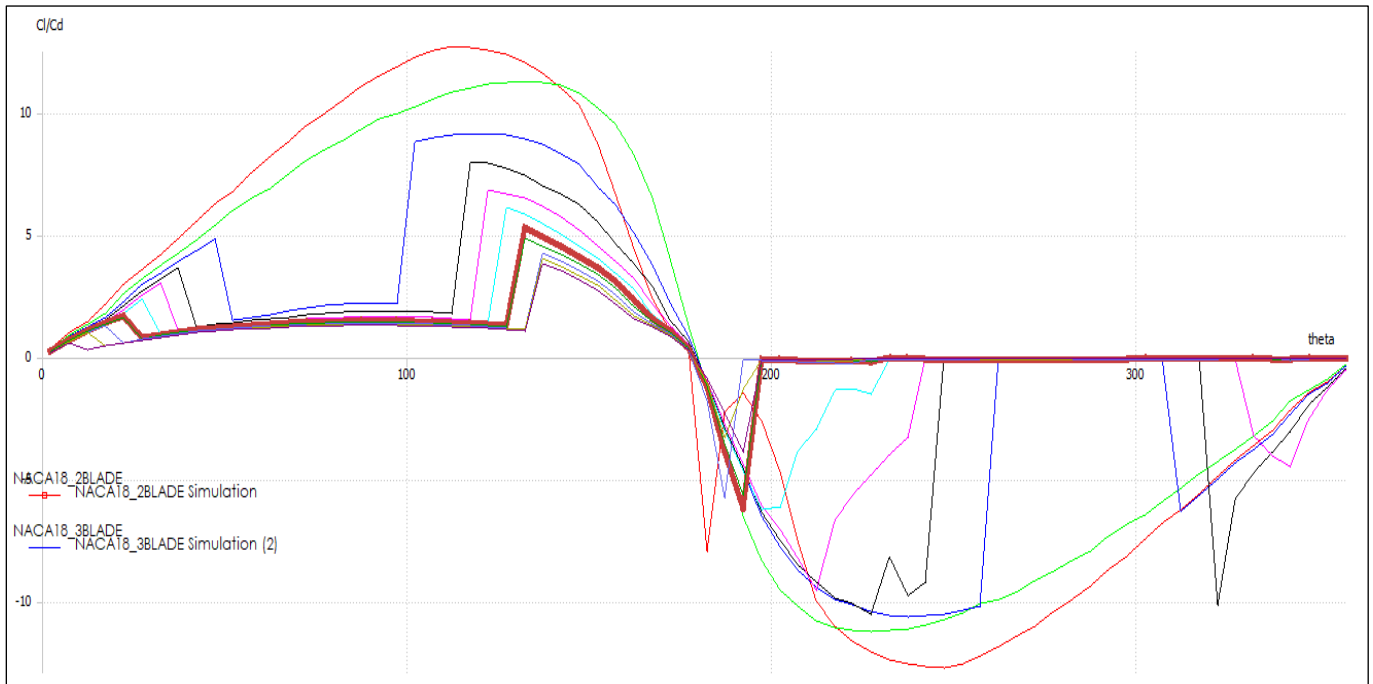


Figure 32. Cl/Cd vs theta plot of top-section for TSR 4

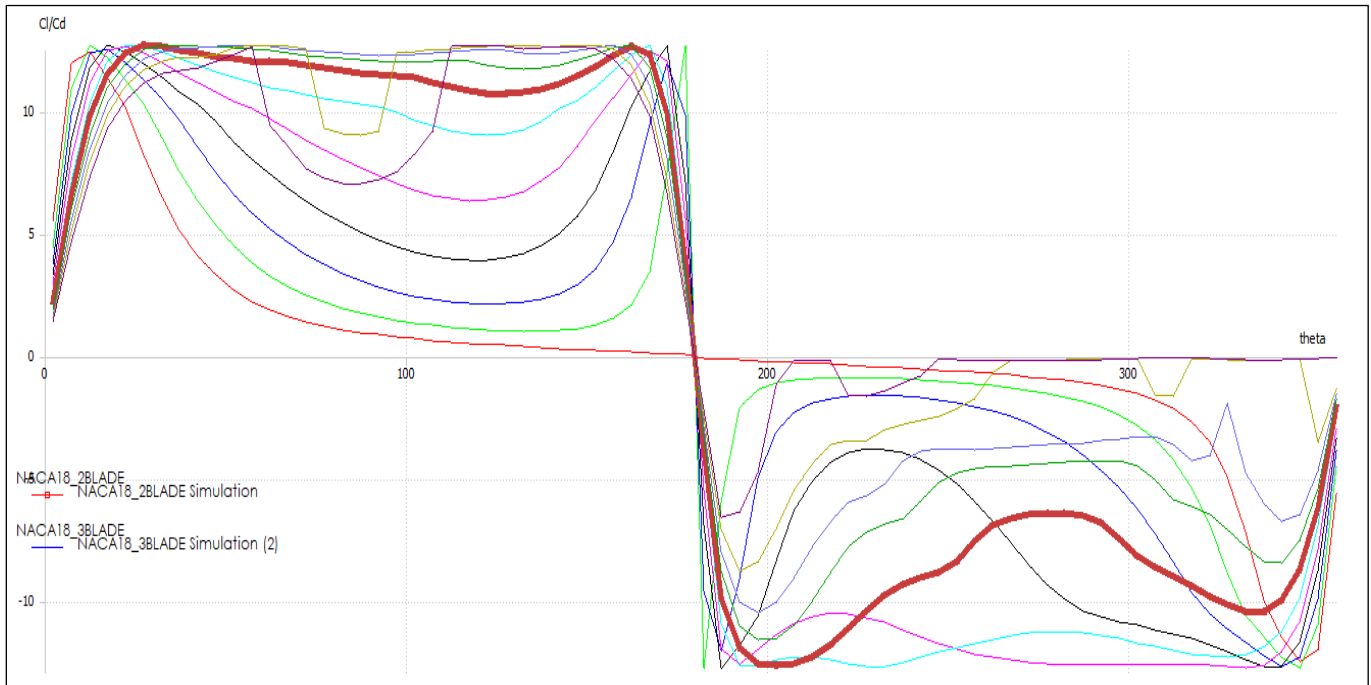


Figure 33. CI/Cd vs theta plot of mid-section for TSR 4

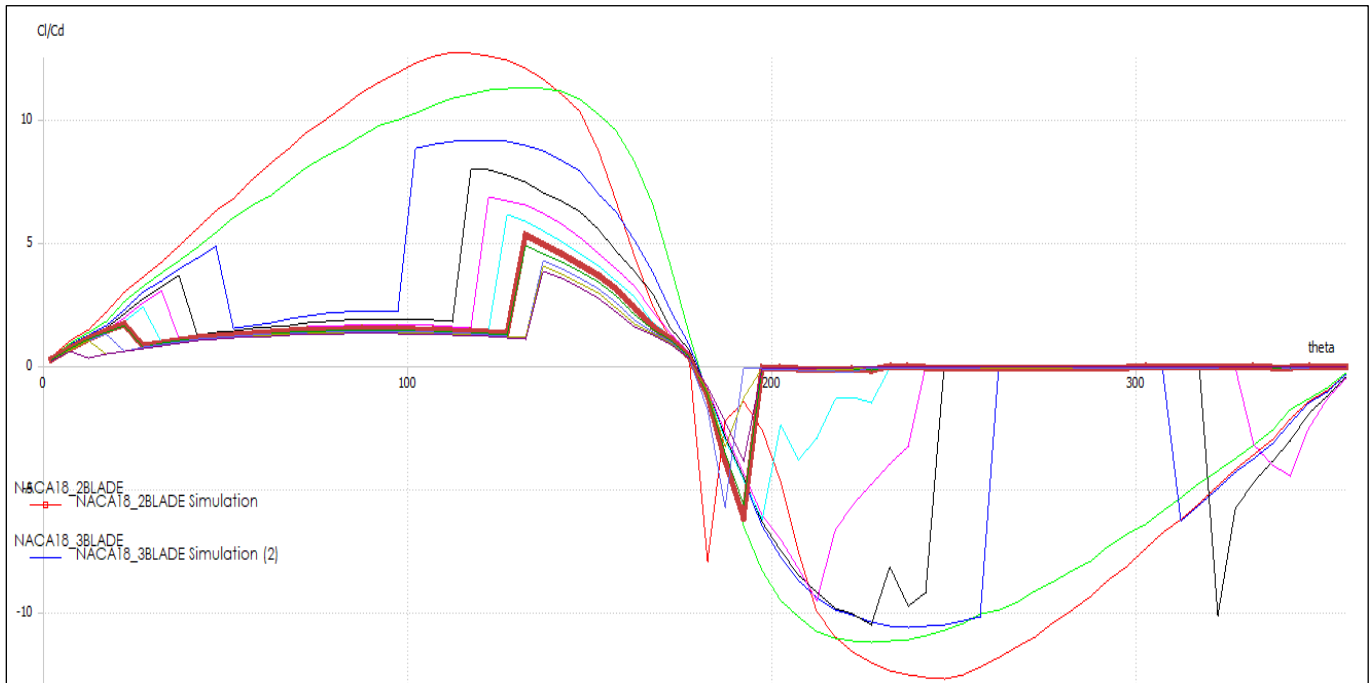


Figure 34. CI/Cd vs theta plot of bottom-section for TSR 4

#### 4.2.2.5. TSR 5

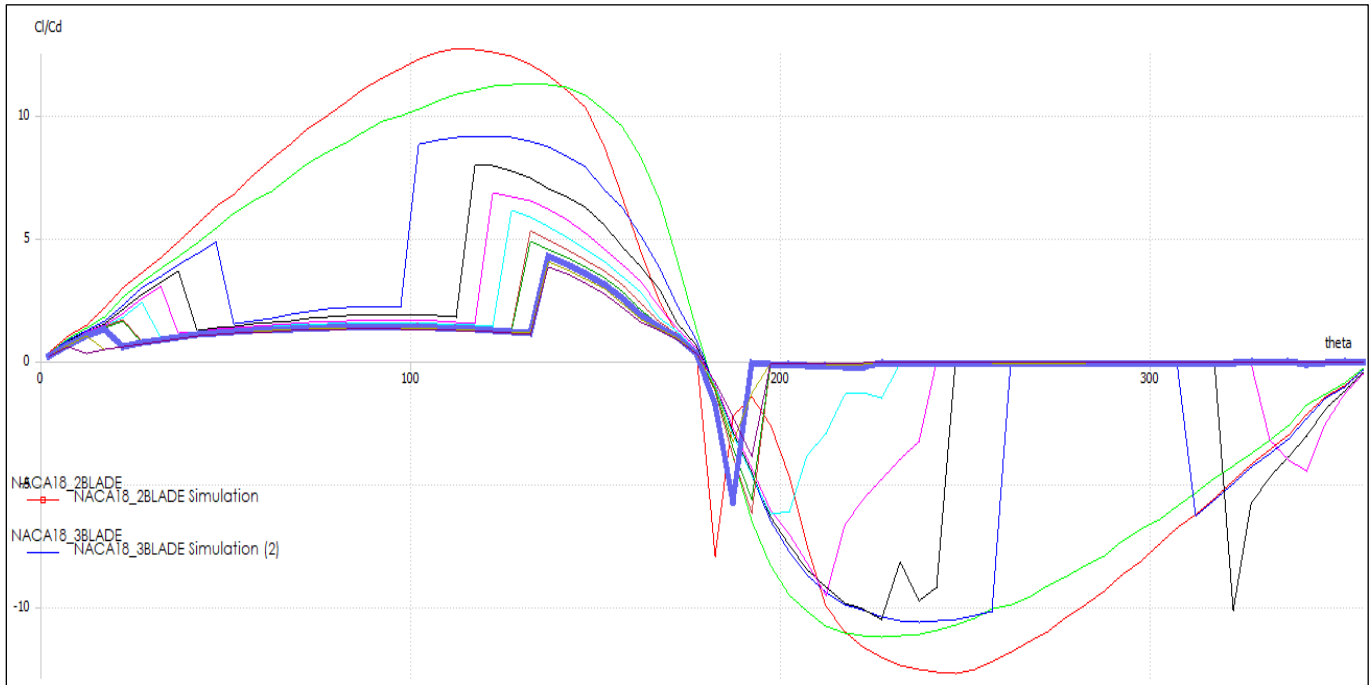


Figure 35. Cl/Cd vs theta plot of top-section for TSR 5

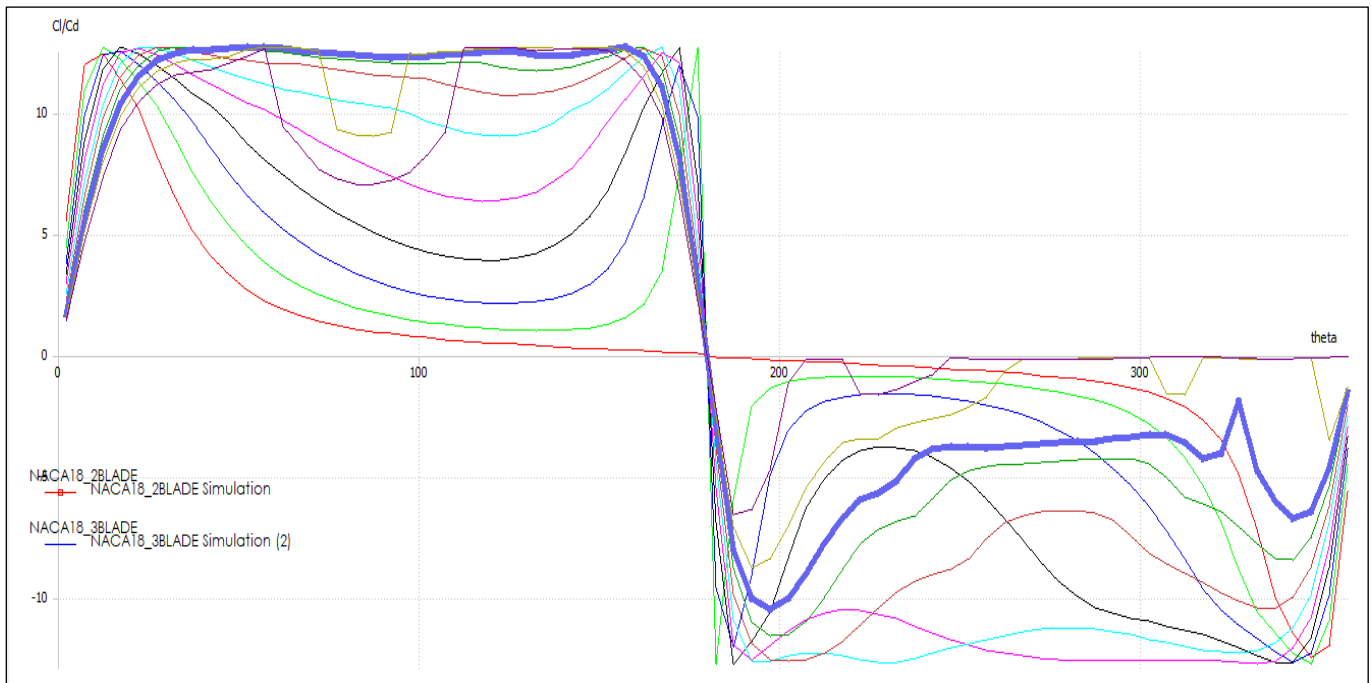


Figure 36. Cl/Cd vs theta plot of mid-section for TSR 5

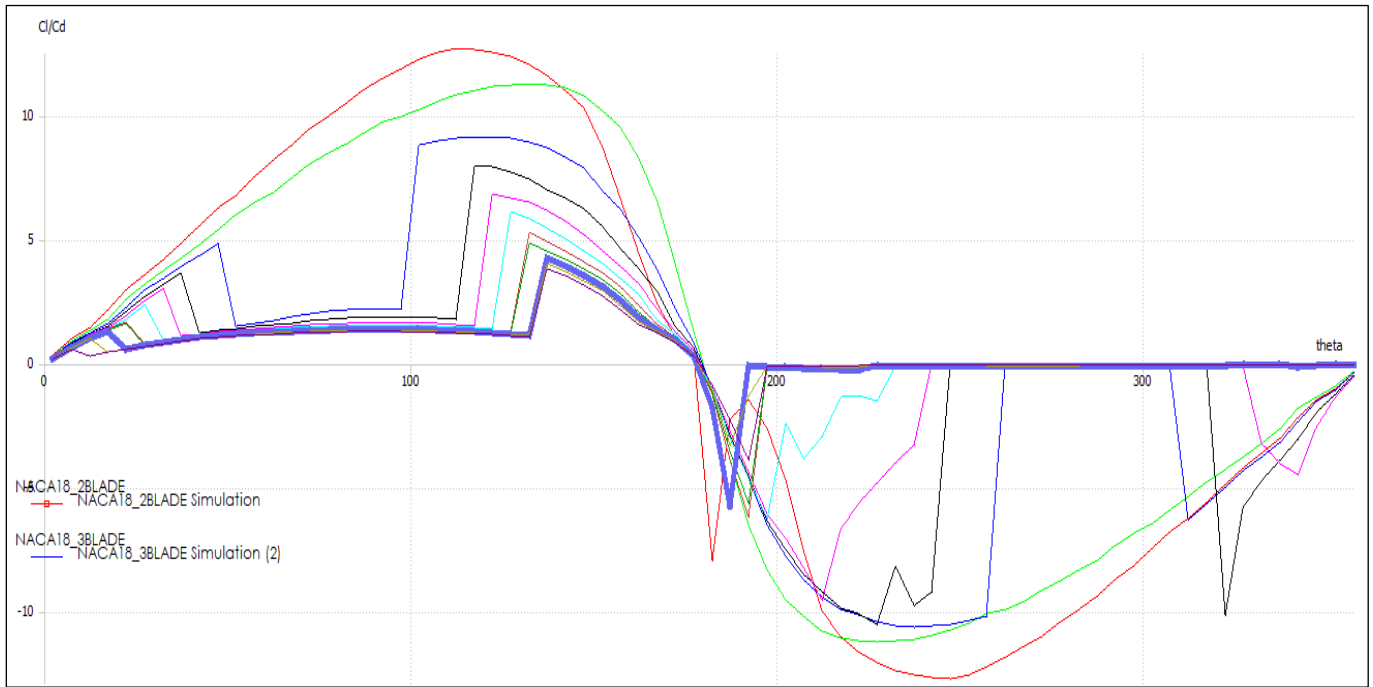


Figure 37. Cl/Cd vs theta plot of bottom-section for TSR 5

#### 4.2.2.6. TSR 6

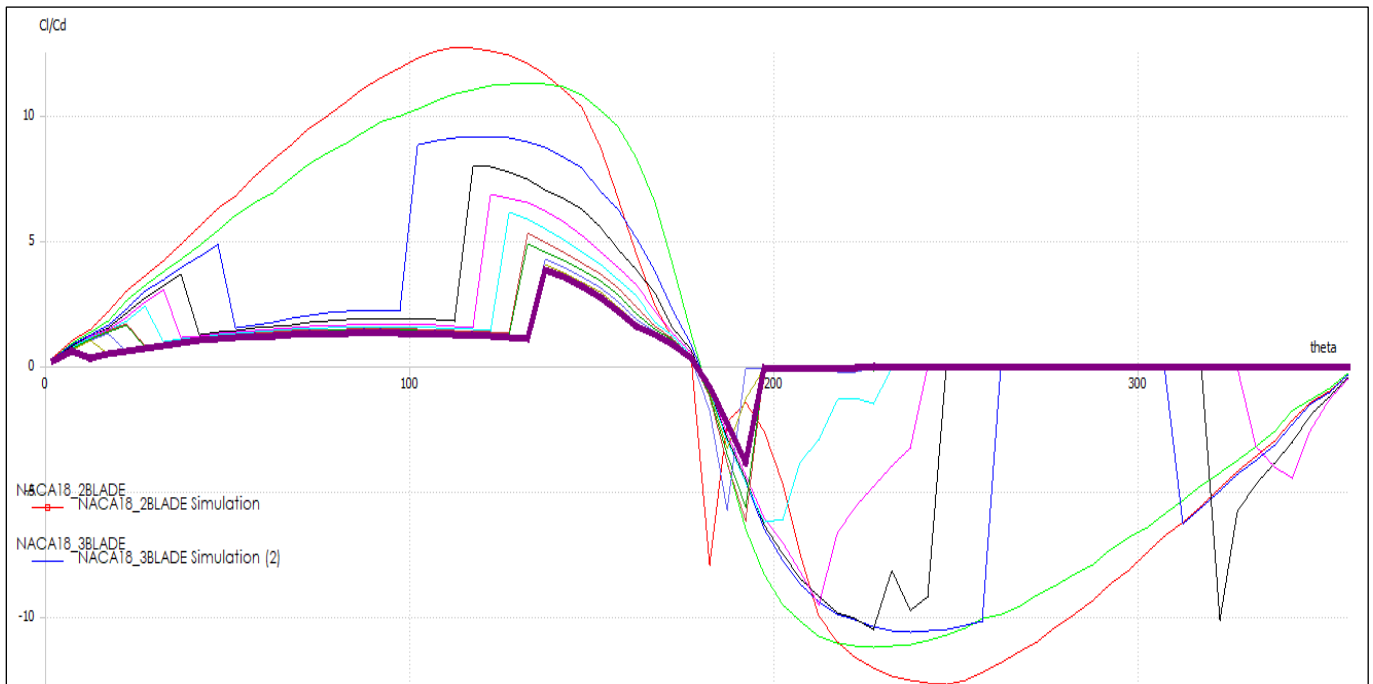


Figure 38. Cl/Cd vs theta plot of top-section for TSR 6

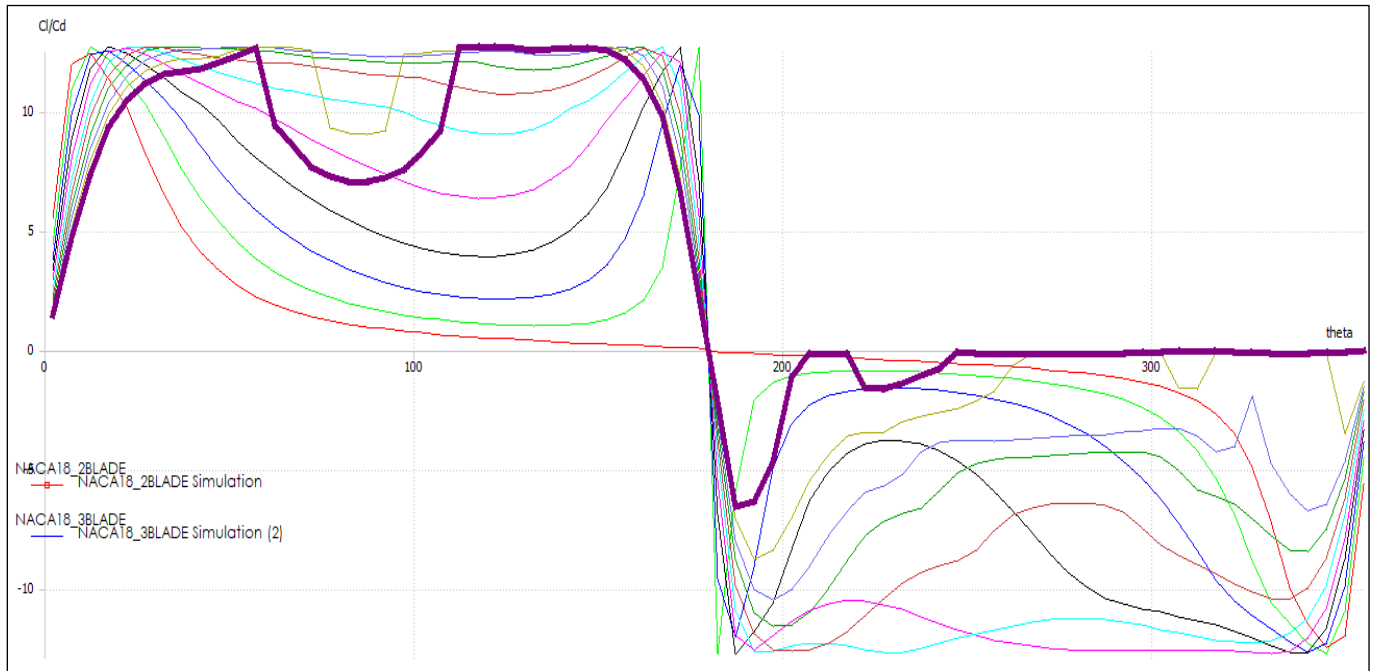


Figure 39. CI/Cd vs theta plot of mid-section for TSR 6

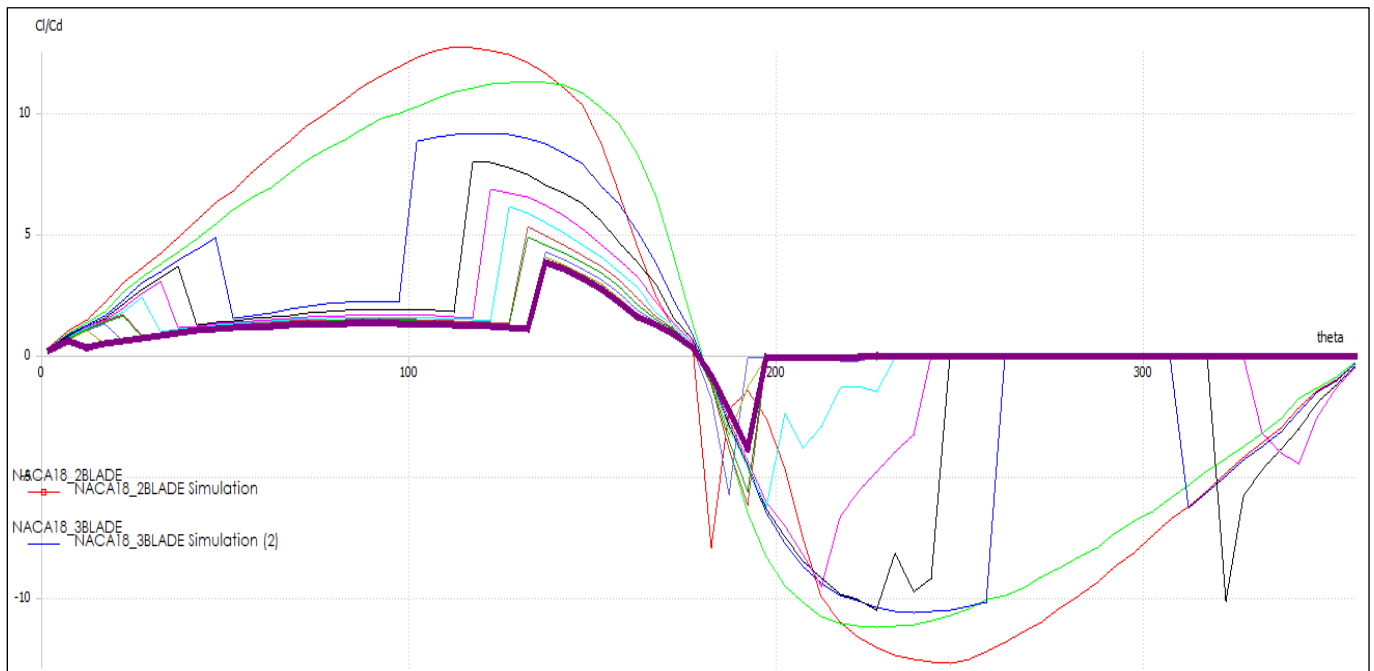


Figure 40. CI/Cd vs theta plot of bottom-section for TSR 6

#### 4.2.3. Comparative study of two-bladed and three-bladed models

From the above it can be concluded that the working TSR for both the types of turbine under study is between TSR 3 to TSR

4. Henceforth the below study will be broadly focused on the above conclusion itself for better understanding the comparative analysis between the two models. Figures 41 and 43 suggest the improvement in the performance when the variable pitch model is applied compared to a fixed pitch



method. The further discussion arises is the impact on performance with an increase in several blades in the VAWT model used for the investigation.

As anticipated, if related to two-bladed turbines, three-bladed wind turbines display better efficiency. As a result, it also reports a higher thrust. Together with a two-bladed, a smaller variance in both torque and thrust also occurs. These actions may reflect a significant benefit for simple, three-bladed VAWT systems, over which the increased expense of manufacture and installation is just not as significant as for larger rotors. The number of blades has major effects on load parameters as can be seen from the following results. But also guide towards the best fit range for the tip speed ratio.

In addition, the calculations suggested that have used the airfoil NACA0018 indicate improved rotor efficiency when

beginning TSRs (at low rotor level, minimizing VAWT start-up issues), but mostly a pronounced restriction in the usage of wind energy at low to moderate wind speeds, representative of the urban neighborhood. The three-blade model gives more power and is more stable compared to a two-blade model. Also for lower tip speed ratio, the performance of three-blades is better, but it decreases as the tip speed ratio gradually increases.

#### 4.2.3.1. $C_m$ vs TSR

Figure 41 shows plot  $C_m$  versus TSR, the output for three-bladed is better than the two-bladed in TSR range under consideration but if the turbine is performing beyond this range i.e.  $TSR > 4$  its seen two-bladed turbine performing at par to that of three-bladed turbine.

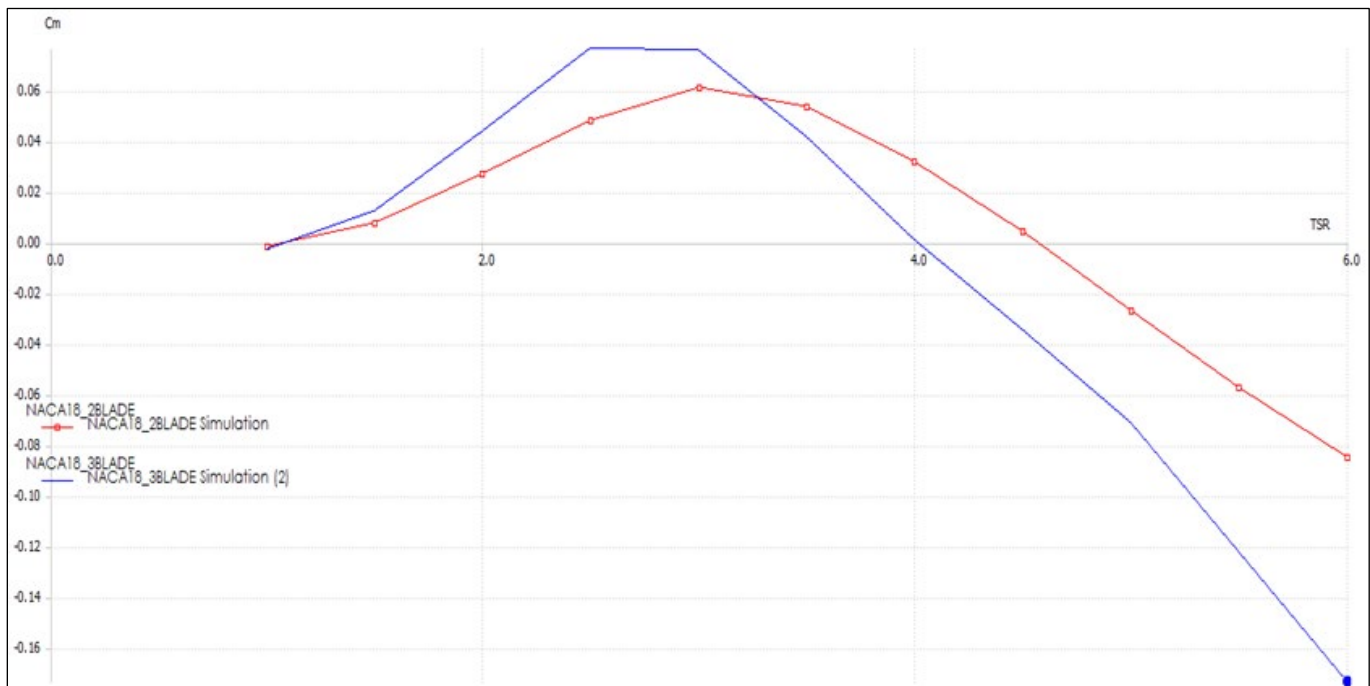


Figure 41.  $C_m$  vs TSR

#### 4.2.3.2. $C_p$ vs TSR

Figure 42 is a representation of analysis between  $C_p$  and TSR, the performance of the three-bladed turbines is better in the optimum TSR range. The maximum attend value of TSR is 0.22 by the three-bladed turbine whereas the two-bladed turbine  $C_p$

values lie under 0.2 only. It shows a better performance of 15.78 % more than the two-bladed turbines with variable pitch system. For lower TSR three-bladed wind turbines perform better comparatively.

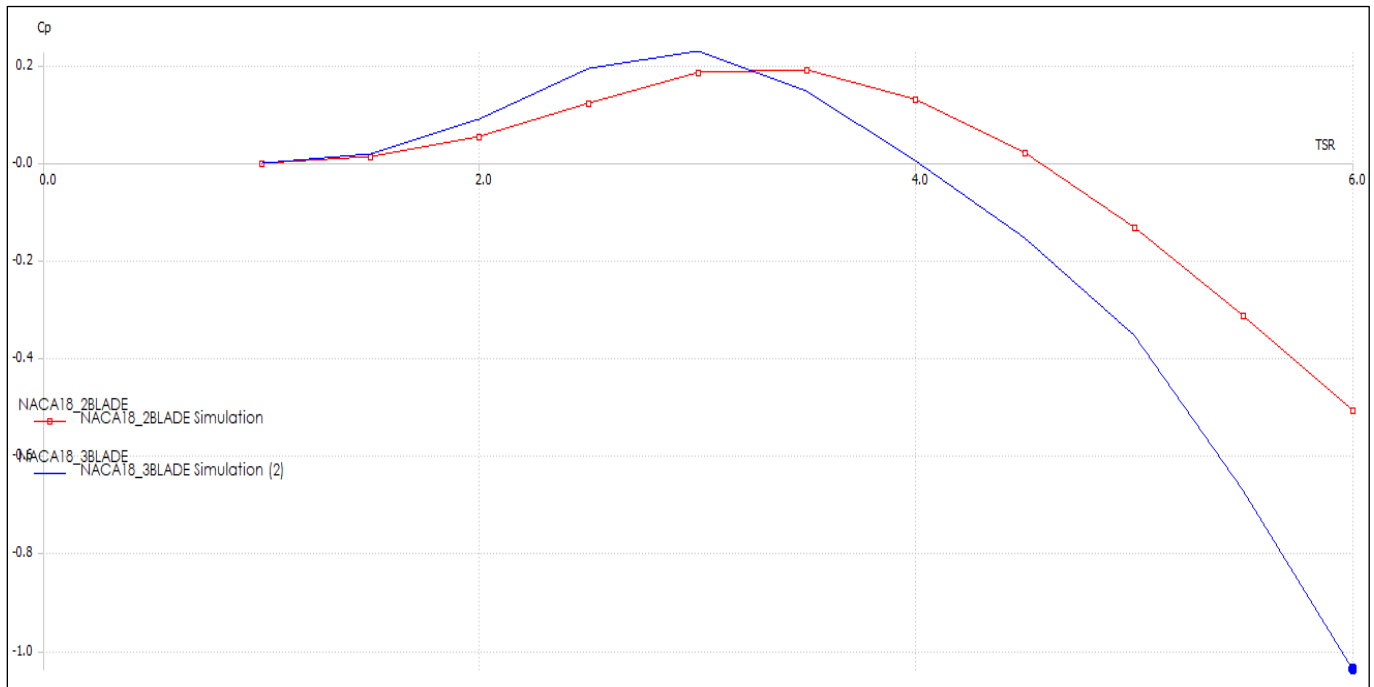


Figure 42. Cp vs TSR

### 4.2.3.3. Cp vs Wind speed

Figure 43 shows the plot of Cp versus wind speed and the Cp attained is similar to two-bladed, the value of Cp decreases with the increase in speed of the wind. But here also as it can be

noted the value of Cp for three-bladed is higher than the two-bladed turbine systems.

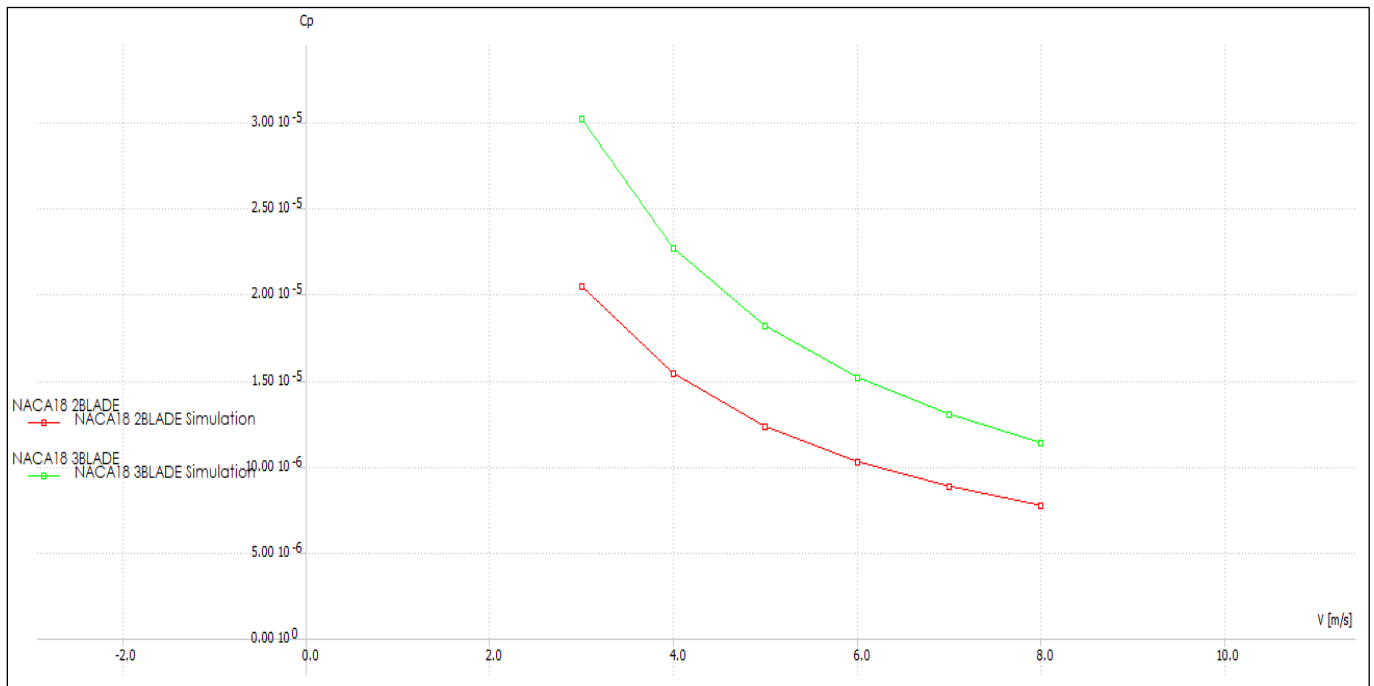


Figure 43. Cp vs Wind speed

#### 4.2.3.4. Power vs wind speed and Torque vs wind speed

Figure 44 and figure 45 give the power versus wind speed plot and torque versus wind speed plot respectively. Both power and torque shows an increasing trend with an increase in wind speed. Both of the plots the rate of increase is steeper for the

three-bladed system. Thus it can be concluded that with an increase in the number of blade torque transmitted to the shaft as well increases.

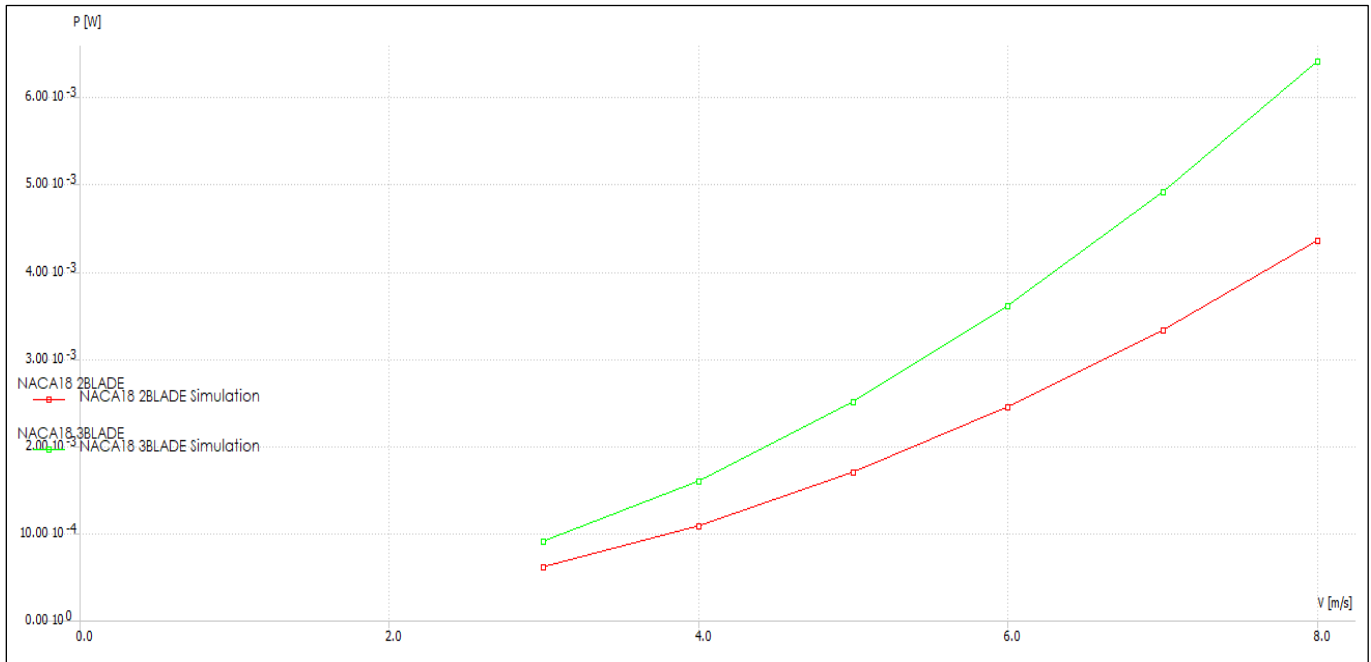


Figure 44. Power vs wind speed

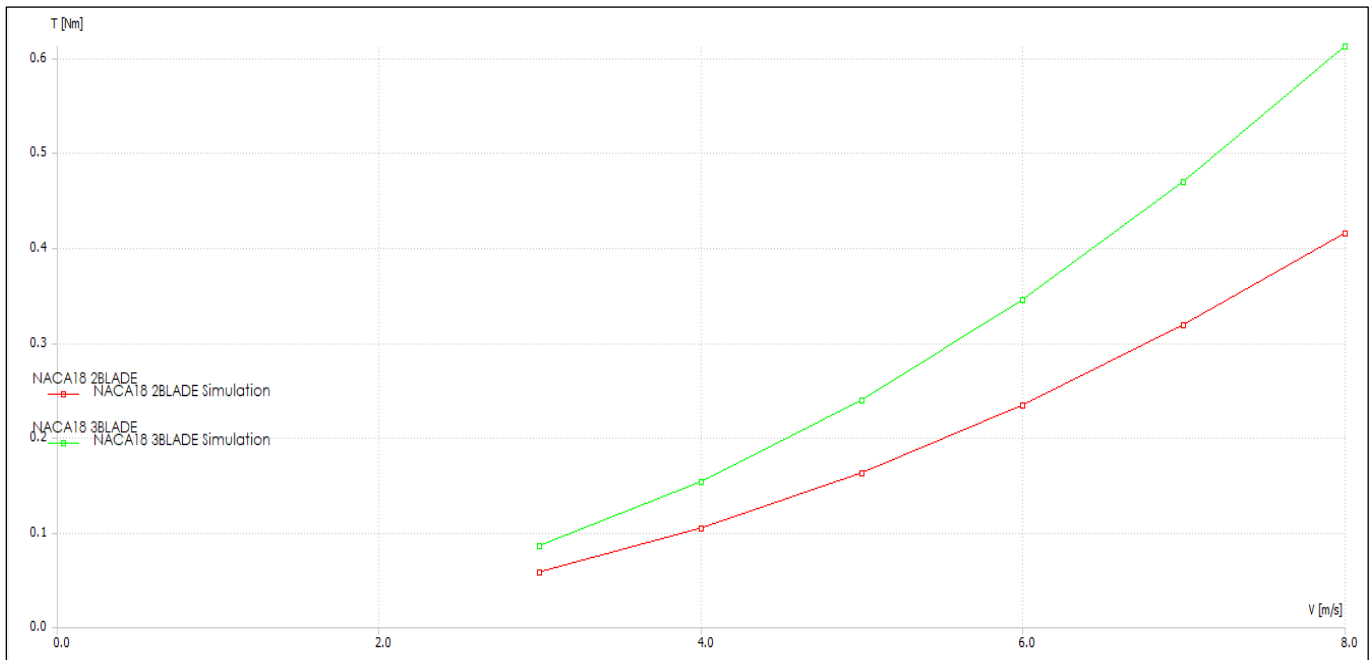


Figure 45. Torque vs wind speed

### 4.2.3.5. Thrust vs TSR

Figure 46 is a plot between the thrust force and TSR. It can be seen from the plot that the thrust increases from TSR 1 to TSR 5, and there is a fall in thrust from 24 Nm to 19 Nm, it can be

due to turbulence created in the turbine at high speed, hence it also indicate that the turbine works well under the TSR below 5.

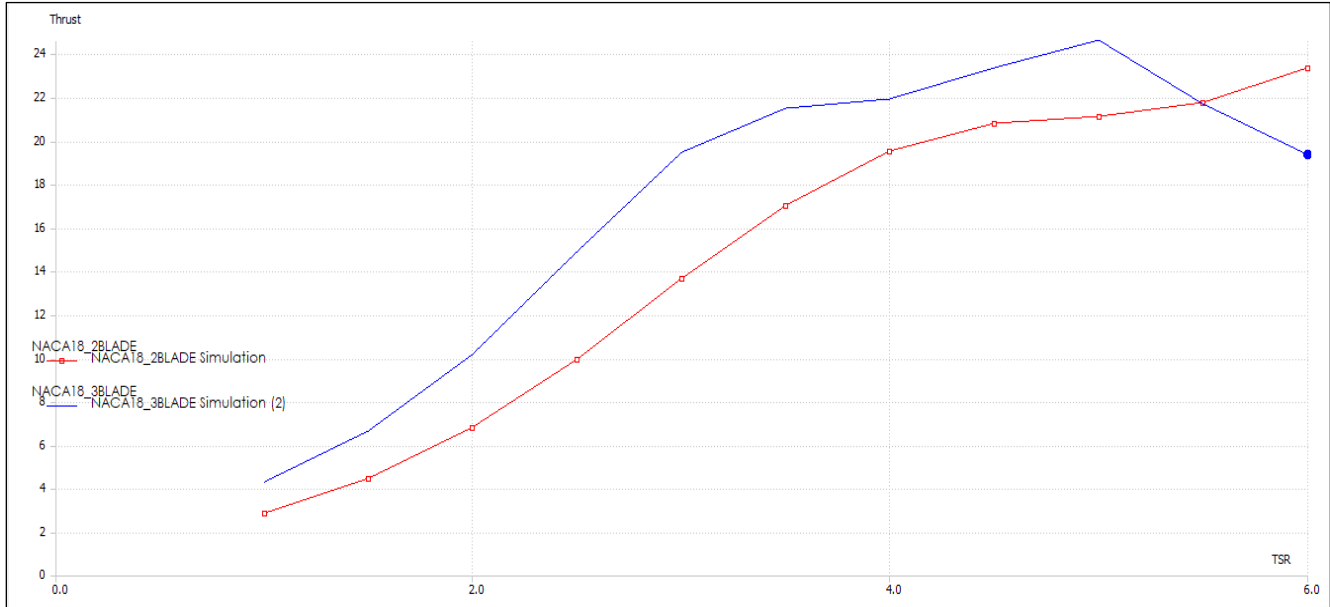


Figure 46. Thrust vs TSR

### 4.2.4. Simulation

#### 4.2.4.1. Two-bladed turbine vortex simulations

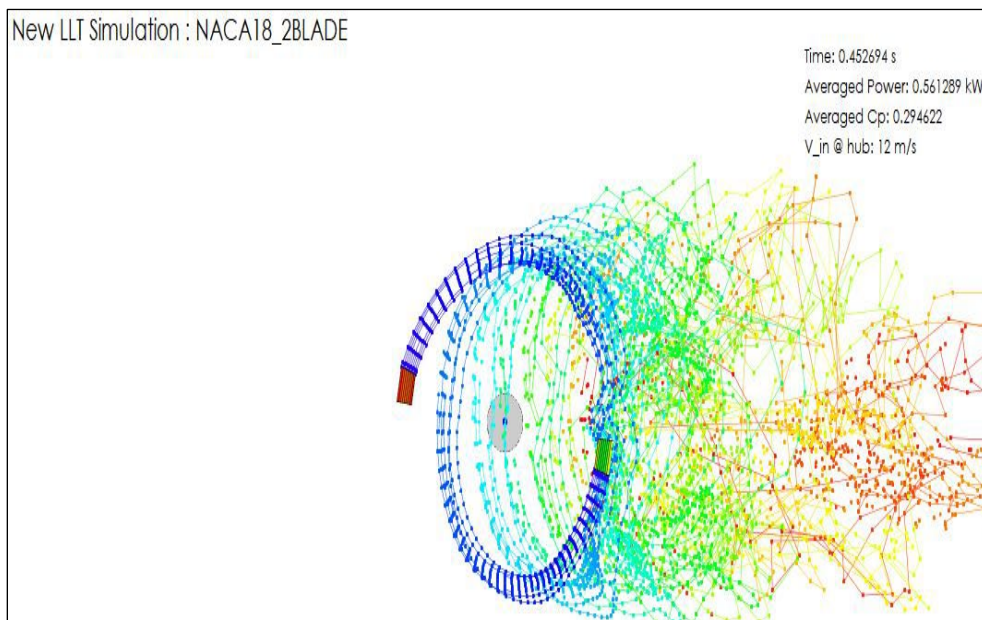
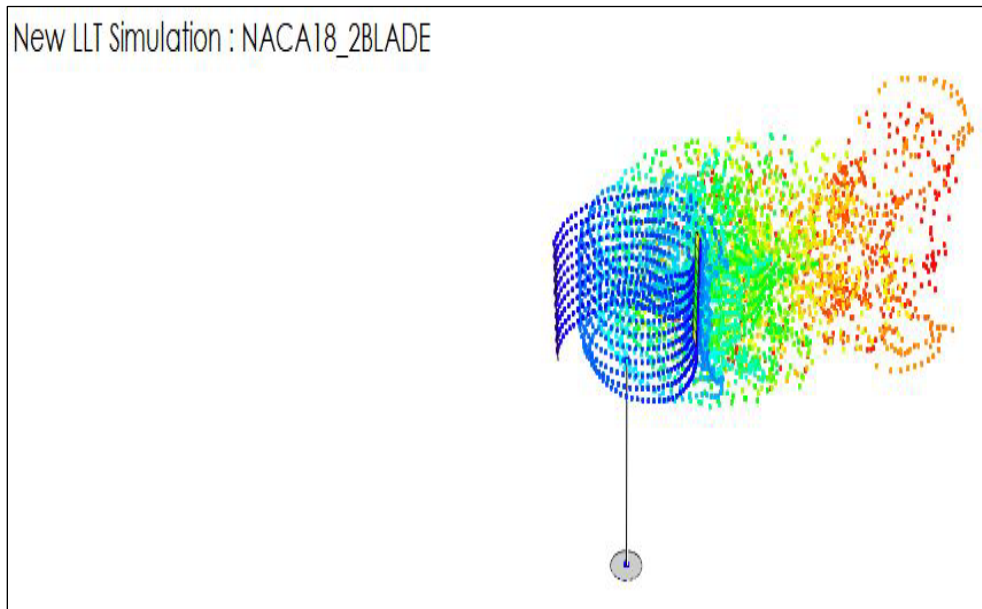


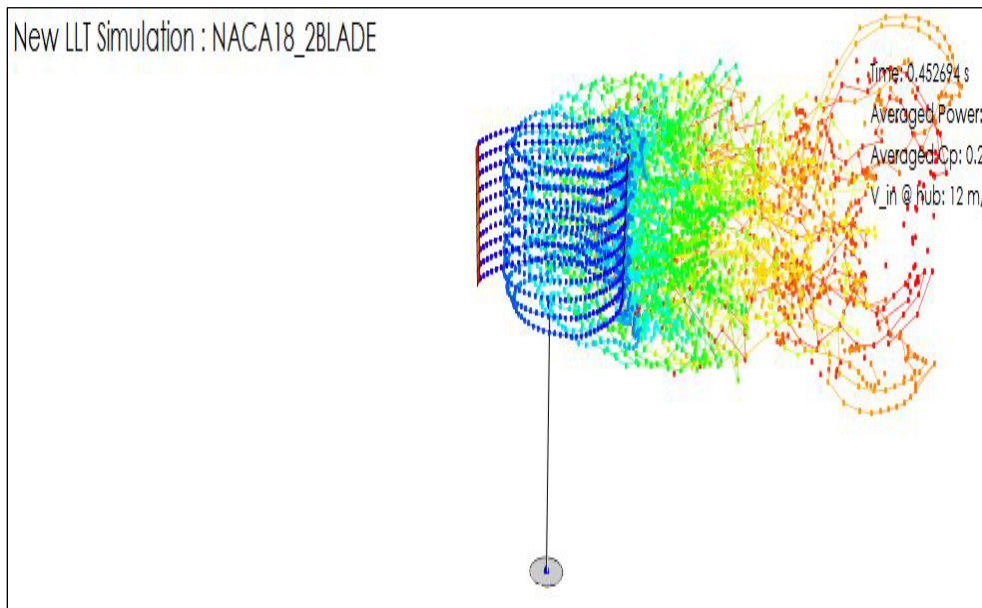
Figure 47. Two-bladed vortex simulation 1

Figure 48 shows vortex nodes with passage of time and no trailing vortex has here been depicted. Figure 49 gives the illustration of the simulation with trailing vortices, with vortex shredding and vortex nodes. Figure 47 to figure 49 shown below gives a better depiction of the working situation inside two-bladed model of Darrieus VAWT. The series of figure

depicts different vortex conditions so that one can understand what is happening in the flow. Figure 47 gives an image of the model with trailing vortices shown by lines, vortex nodes shown by dots without vortex shredding. The length of the lines shows the aging of the vortex generated by the blades.



**Figure 48.** Two-bladed vortex simulation 2



**Figure 49.** Two-bladed vortex simulation 3

#### 4.2.4.2. Velocity simulation of two-bladed turbines

The small dashed lines give vector components of velocity at each point. But the simulation of QBlade software gives

distribution around the whole of the rotor domain, which is again an advantage as it will help in analyzing the flow wind through the rotor domain as well and just the blade. Figure 52 gives velocity distribution across the blade as well as in the rotor domain as well. The color depicts the velocity distribution inside the rotor and across the blade profile.

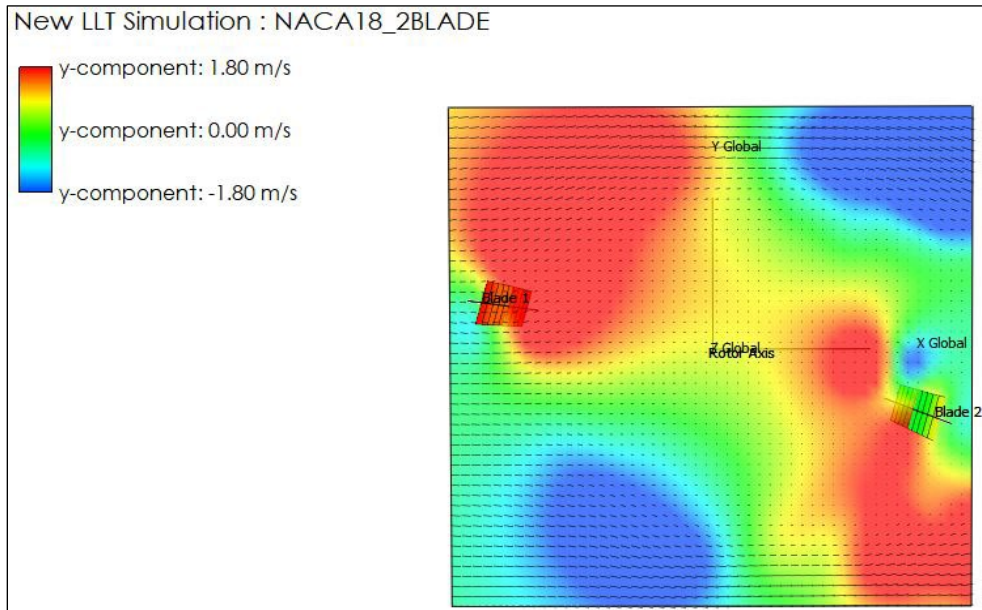


Figure 50. Two-bladed velocity simulation

#### 4.2.4.3. Three-bladed turbine vortex simulation

Figure 51 gives a vortex simulation of a three-bladed turbine with no shredding and no trailing vortices. Figure 52 gives the

vortex simulation with trailing vortices, along with vortex shredding phenomena with flow across the turbine rotor.

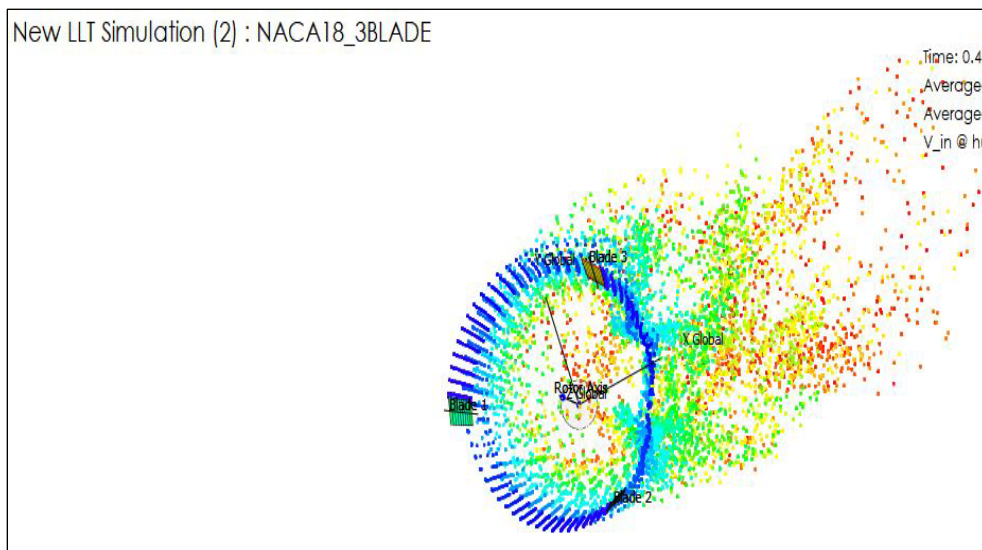


Figure 51. No shredding and trailing vortex simulation

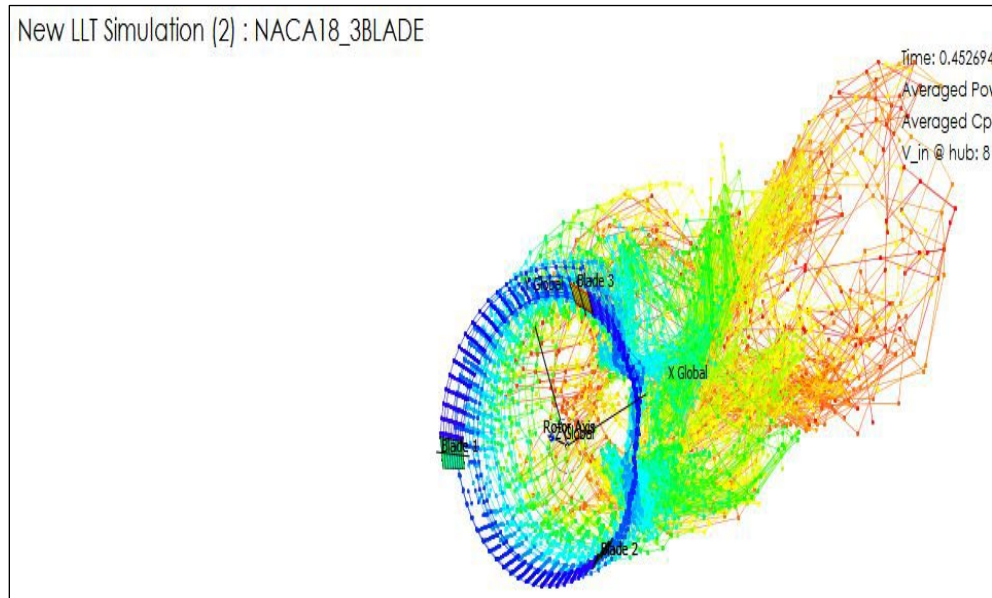


Figure 52. All effects vortex simulation

#### 4.2.4.4. Three-bladed turbine Velocity simulation

The small dashed lines give vector components of velocity at each point. The image is similar to the one taken from the paper. Figure 53 gives velocity distribution across the blade as

well as in the rotor domain as well. The color depicts the velocity distribution across the different regions of the turbine and across the blades.

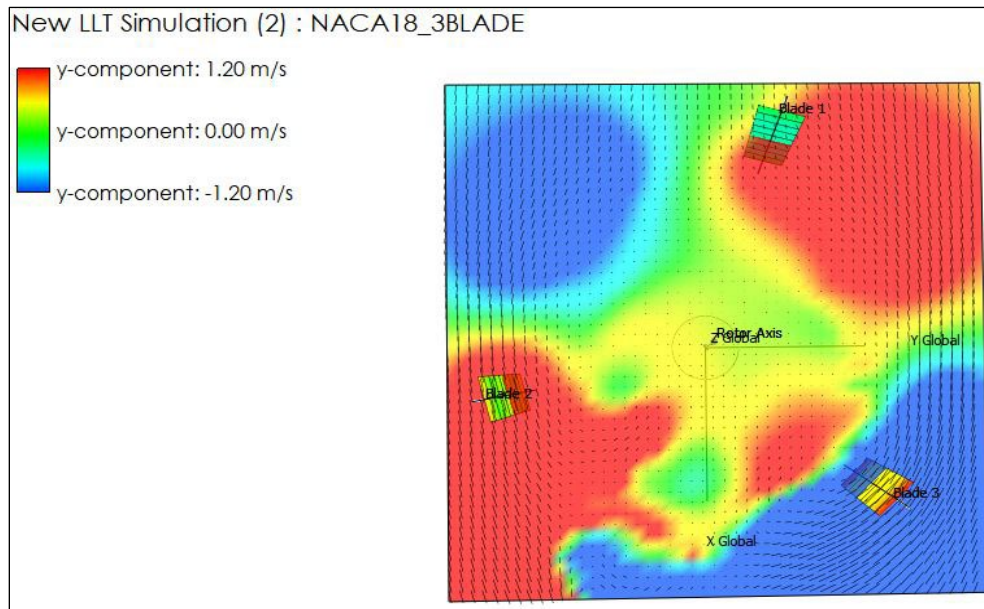


Figure 53. Three-bladed turbine velocity simulation

### 4.3. Discussions

Figure 7 to 10, show the share of contribution of different sections of blades towards power generation of the turbine as a whole. It can be concluded that the mid-region of the turbine

has the maximum contribution towards the share of power; the trapezoidal shape gives a larger area, which signifies a larger greater contribution in lift by this portion. The shares of the top and bottom regions have little contribution to the lift force in working. This brings to the future work for further investigation

of various designs modification at the top and bottom zone, which will enhance the self-starting capacity of a turbine and increase the contribution of these regions in power and lift contribution of the turbine. The proposed analysis deploying the DMST approach using QBlade software gives quick convergence with a reasonable number of iteration. The analysis indicates the performance of the turbine at TSR 4 to be most effective for the variable pitch approach of the two-bladed turbines under the observation. The steep decline in the coefficient of power and coefficient of moment parameter of turbine beyond TSR 4 further assure the working it be optimal TSR.

## 5. Conclusions

The paper is based on the simulation of the turbine model of NACA0018 airfoil blades for variable pitch between (-10 degree to +10 degree). The study was carried using the QBlade software which is a BEM based approach. The following results can be concluded-

1. Losses incurred at the top and bottom edges of the turbine are high and the future scope of work requires design modification for reducing these losses.
2. An increment in  $C_p$  is observed  $1 < \text{TSR} < 3.5$ , beyond TSR 4.0, decrement is observed with variable pitch gives improved power coefficient for slow speed wind turbine.
3. The performance of the turbine is optimum in the TSR range between 3 and 4 for both types of turbines in consideration.
4. The BEM gives a good correlation of the results and proves to be an effective tool for quick analysis of VAWT.
5. To select a suitable and efficient wind turbine computational analysis will be carry out where the computational model will be selected. For any experimental or field work, advanced analysis plays a vital role where QBlade software can be used.

## 6. Future scope

Generally the analysis is carried out in CFD tools which take more time, and are costly but using QBlade, open source software minimized computation time. Future scope of the present work are given below

- The study of effect of the blade twist angle in the blade, and studying the variable pitch effect on performance of the turbine.
- Simulation of the different parameters on the performance of turbine when variable pitch is employed.

## Acknowledgements

The author would like to thank the authority of Visvesvaraya Institute of Technology, Nagpur for providing this opportunity to carry forward this research.

## References

- [1] Balat, M. (2009). A review of modern wind turbine technology. *Energy Sources, Part A*, 31(17), 1561-1572.
- [2] Kumara, E. A. D., Hettiarachchi, N., and Jayathilake, R. (2017). Overview of the vertical axis wind turbines. *Int. J. Sci. Res. Innov. Technol*, 4, 56-67.
- [3] Wang, Z., Bui, Q., Zhang, B., and Pham, T. L. H. (2020). Biomass energy production and its impacts on the ecological footprint: An investigation of the G7 countries. *Science of the Total Environment*, 743, 140741.
- [4] Patlins A, A. S., and Hnatov, A. (2018). Determination of the Best Load Parameters for Productive Operation of PV Panels of Series FS-100M and FS-110P for Sustainable Energy Efficient Road Pavement: 2018 IEEE 59th International Scientific Conference on Power and Electrical Engineering of Riga Technical University (RTUCON 2018): Conference Proceedings, 12 Nov. 2018. Riga: RTU, 1-6.
- [5] Zhu, Y., Li, K., Liu, C., and Mgijimi, M. B. (2019). Geothermal Power Production from Abandoned Oil Reservoirs Using In Situ Combustion Technology. *Energies*, 12(23), 4476.
- [6] Singhal, A. (2020). Biofuels: Perspective for Sustainable Development and Climate Change Mitigation. In *Biotechnology for Biofuels: A Sustainable Green Energy Solution* (pp. 1-22). Springer, Singapore.
- [7] Hnatov, A., Arhun, S., Dziubenko, O., and Ponikarovska, S. (2018). Choice of electric engines connection circuits in electric machine unit of electric power generation device. *Majlesi Journal of Electrical Engineering*, 12(4), 85-93.
- [8] Paraschivoiu, I., Trifu, O., and Saeed, F. (2009). H-Darrieus wind turbine with blade pitch control. *International Journal of Rotating Machinery*, 2009.
- [9] Krishna, J. M., Bhargava, V., and Donepudi, J. (2018). BEM Prediction of Wind Turbine Operation and Performance. *International Journal of Renewable Energy Research*, 8(4).
- [10] Elsakka, M. M., Ingham, D. B., Ma, L., and Pourkashanian, M. (2019). CFD analysis of the angle of attack for a vertical axis wind turbine blade. *Energy Conversion and Management*, 182, 154-165.
- [11] Zhao, Z., Wang, R., Shen, W., Wang, T., Xu, B., Zheng, Y., and Qian, S. (2018). Variable pitch approach for performance improving of straight-bladed VAWT at rated tip speed ratio. *Applied Sciences*, 8(6), 957.
- [12] Vaz, J. R. P., Pinho, J. T., and Mesquita, A. L. A. (2011). An extension of BEM method applied to horizontal-axis wind turbine design. *Renewable Energy*, 36(6), 1734-1740.
- [13] Chandramouli, S., Premsai, T. P., Prithviraj, P., Mugundhan, V., and Velamati, R. K. (2014). Numerical analysis of effect of pitch angle on a small scale vertical axis wind turbine. *International Journal of Renewable Energy Research (IJRER)*, 4(4), 929-935.
- [14] Rogowski, K., Hansen, M. O., and Maroński, R. (2018). Steady and unsteady analysis of NACA0018 airfoil in vertical-axis wind turbine. *Journal of Theoretical and Applied Mechanics*, 56.



- [15] Rogowski, K., Hansen, M. O. L., and Lichota, P. (2018). 2-D CFD Computations of the two-bladed darrieus-type wind turbine. *Journal of Applied Fluid Mechanics*, 11(4), 835-845.
- [16] Habtamu, B., and Yingxue, Y. (2011). Double multiple stream tube model and numerical analysis of vertical axis wind turbine. *Energy and Power Engineering*, 3, 262-270.
- [17] Q-blade.org. 2020. QBlade. [online] Available at: <<http://www.q-blade.org>> [Accessed 9 September 2020].
- [18] Moghimi, M., and Motawej, H. (2020). Developed DMST model for performance analysis and parametric evaluation of Gorlov vertical axis wind turbines. *Sustainable Energy Technologies and Assessments*, 37, 100616.
- [19] Vergaerde, A., De Troyer, T., Molina, A. C., Standaert, L., and Runacres, M. C. (2019). Design, manufacturing and validation of a vertical-axis wind turbine setup for wind tunnel tests. *Journal of Wind Engineering and Industrial Aerodynamics*, 193, 103949.
- [20] Rogowski, K. Hansen, M and Lichota, P. (2018). 2-D CFD computations of the two-bladed darrieus-type wind turbine, *Journal of Applied Fluid Mechanics*, 11(4), 835-845.
- [21] Vergaerde, A., Troyer, T. D, A. Molina, C., Standaert, L. and Runacres, M. (2019). Design, manufacturing and validation of a vertical-axis wind turbine setup for wind tunnel tests, *Journal of Wind Engineering and Industrial Aerodynamics*, 193, 103943.
- [22] Mazarbhuiya, H. M. S. M., Biswas, A., and Sharma, K. K. (2020). A 2D numerical simulation of blade twist effect on the aerodynamic performance of an asymmetric blade vertical axis wind turbine in low wind speed. *EAI Endorsed Transactions on Energy Web*, 7(28), 1-7.